Accepted Manuscript

Electrodeposition and electrodissolution of zinc in mixed methanesulfonate-based electrolytes

Kiana Amini, Mark D. Pritzker

PII: S0013-4686(18)30382-7

DOI: 10.1016/j.electacta.2018.02.087

Reference: EA 31282

To appear in: *Electrochimica Acta*

Received Date: 14 September 2017

Revised Date: 12 January 2018

Accepted Date: 17 February 2018

Please cite this article as: K. Amini, M.D. Pritzker, Electrodeposition and electrodissolution of zinc in mixed methanesulfonate-based electrolytes, *Electrochimica Acta* (2018), doi: 10.1016/j.electacta.2018.02.087.

Electrodeposition and Electrodissolution of Zinc in Mixed Methanesulfonate-Based Electrolytes

Kiana Amini, Mark D. Pritzker*

Department of Chemical Engineering, University of Waterloo, 200 University Avenue West, Waterloo, Ontario, Canada N2L 3G1

Abstract

Zinc electrodeposition and electrodissolution in methanesulfonic acid (MSA) electrolytes mixed with chloride or sulfate are investigated in a 3-electrode cell for eventual use in divided and undivided zinc-cerium redox flow batteries (RFB). Cyclic voltammetry and polarization experiments show that the addition of chloride to methanesulfonate-based electrolytes shifts the nucleation potential in the positive direction, lowers the nucleation overpotential and enhances the kinetics of Zn deposition and subsequent dissolution relative to that achieved when sulfate is added or MSA is the only anion present. In addition, the diffusion coefficient of Zn(II) and the resulting limiting current density for Zn deposition have been found to be moderately higher in mixed methanesulfonate/chloride media than when chloride is absent. The effects of temperature, MSA concentration, Zn(II) concentration and current density on the Zn/Zn(II) system have also been investigated under potentiostatic and galvanostatic conditions. Although an increase in temperature and/or MSA concentration tends to lower the charge efficiency for Zn deposition in both mixed and MSA-only electrolytes due to the higher rate of hydrogen evolution, the amount of zinc deposited, charge and voltage efficiency always remain significantly higher in the mixed methanesulfonate/chloride media than the pure MSA media. Thus, the use of a mixed methanesulfonate/chloride media should enable both divided

*Corresponding author. Tel.: +1 519 888 4567 x32542
Email address: pritzker@uwaterloo.ca (Mark D. Pritzker)

and undivided zinc-cerium RFBs to operate over a wider range of temperatures and MSA concentrations compared to the case with pure MSA electrolyte. The addition of sulfate to MSA-based electrolytes, however, does not improve the performance of the Zn/Zn(II) system relative to that possible in the MSA-only electrolytes.

Keywords: deposition, dissolution, mixed electrolyte, redox flow battery, zinc

1. Introduction

In the last few years, the interest in energy storage devices has intensified [1,2]. A reliable and cost-effective energy storage unit can dramatically enhance the integration of renewable energies such as solar and wind into the electrical grid and can smooth out the large inherent fluctuations in the availability of these sources. The energy produced from renewable sources under the proper conditions (time and climate) can be stored in a storage unit and discharged during periods of high demand. If successful, these storage devices will enable the electrical grid to be far less reliant on energy sources such as fossil fuels that are responsible for major environmental problems (climate change, acid rain, air pollution).

One of the most recent and promising technologies for energy storage are redox flow batteries (RFB). Since the active material in RFBs is stored externally from the cell in storage tanks, the energy and power of such batteries are independent and so they can be scaled up more easily than other types of storage devices [3]. Over the past decades, different RFB systems have been developed. Among these systems, zinc-based RFBs have gained a great deal of attention due to the availability and low price of zinc and the successful use of zinc electrodes in many other battery systems. More importantly, the zinc redox couple provides a large negative potential in aqueous media with a two-electron transfer reaction. Zinc-cerium RFBs are relatively new systems developed by Plurion Inc. [4]. This system offers the highest open-circuit voltage (2.4 V) among the other RFBs, which can lead to high energy densities when the elec-

trolyte contains high concentrations of the electroactive species. In this battery, methanesulfonic acid (MSA) has been used as the supporting electrolyte for both the negative Zn/Zn(II) and positive Ce(III)/Ce(IV) half-cells. Divided two-compartment zinc-cerium RFB cells have been operated with 0.8 mol dm^{-3} cerous methanesulfonate dissolved in 4 mol dm^{-3} MSA for the positive half-cell and 1.5 mol dm^{-3} zinc methanesulfonate in 1 mol dm^{-3} MSA for the negative half-cell [5]. Lower MSA concentrations are used in the negative half-cell since higher concentrations lead to lower zinc deposition/dissolution efficiencies due to competition from the hydrogen evolution reaction [6]. This battery has been operated at 40-60°C [7] due to the higher reversibility and improved kinetics of the Ce(III)/Ce(IV) redox couple at higher temperatures [7], [8].

Despite these advantages, the zinc-cerium system faces a number of obstacles that must be overcome if RFBs based on this chemistry are to become commercially feasible. This has led to considerable research activity on this system in recent years. Despite its favourable thermodynamics, the Ce(III)/Ce(IV) redox reaction has sluggish kinetics [7]. The solubility of Ce(III) rises as the MSA concentration is reduced, whereas the solubility of Ce(IV) is affected in the opposite way [9]. Thus, a compromise must be made to maintain high solubility of both cerium species in the electrolyte. In order to improve the reversibility and kinetics of the Ce(III)/Ce(IV) redox couple and solubility of both cerium species, the use of a mixed-electrolyte media has been investigated as a potential remedy [10,11]. The addition of moderate concentrations (0.5 – 1 mol dm^{-3}) of hydrochloric acid to the base MSA electrolyte has been shown to significantly improve the reversibility and kinetics of the Ce(III)/Ce(IV) redox reaction [11]. Moreover, the diffusion coefficient of Ce(III) was also found to be enhanced in these mixed electrolytes [11]. Although the presence of sulfate rather than chloride in mixed methanesulfonate media also has a positive influence on the Ce(III)/Ce(IV) reaction, its effect does not appear to be as strong [11]. One beneficial effect is an increase in the solubility of Ce(IV) to 1.0 mol dm^{-3} in 2 mol dm^{-3} methanesulfonate / 0.5 mol dm^{-3} sulfate solution [10], while it is less than 0.5 mol dm^{-3} in 2.5 mol dm^{-3} pure MSA electrolyte [9]. The introduction

of a mixed acid media has also been used in all-vanadium redox flow batteries and also found to have positive effects [12,13]. A mixed chloride/sulfate electrolyte enhanced the operating temperature range and stability of vanadium species which was attributed to the formation of stable and soluble vanadium-chloride intermediate complexes [14].

Leung et al. have investigated the use of a membrane-less single compartment zinc-cerium RFB [15]. Elimination of the expensive ion-exchange membrane from RFBs is a very attractive option since it would significantly reduce the cost of materials, simplify the design of the battery and reduce the ohmic resistance across the cell. Moreover, the proposed undivided zinc/cerium RFB is operated at room temperature [15], which is more desirable than the 50°C considered for a divided zinc/cerium RFB [5]. As mentioned before, a high MSA concentration is required for a high solubility of Ce(IV) [9], while the efficiency of zinc deposition/dissolution reaction decreases at high MSA concentrations due to excessive hydrogen evolution [6]. Thus, in a membrane-less battery where a single electrolyte is used, a compromise must be made between a high Ce(IV) solubility and high efficiency of the Zn/Zn(II) redox reaction. Consequently, membrane-less zinc-cerium RFBs have been operated at lower acid concentrations ($\sim$ 0.2 $\mathrm{mol\,dm^{-3}}$ – 0.5 $\mathrm{mol\,dm^{-3}}$) and lower Ce concentrations (0.2 $\mathrm{mol\,dm^{-3}}$ – 0.4 $\mathrm{mol\,dm^{-3}}$ Ce(III)) [15,16]. The most successful undivided battery to date has reportedly achieved a current efficiency of 90% and an energy efficiency of 75% at 20 $\mathrm{mA\,cm^{-2}}$ [15].

As mentioned previously, mixed-acid media, particularly MSA-chloride electrolyte, have been shown to significantly enhance the reversibility and kinetics of the Ce(III)/Ce(IV) half-cell reaction [11]. Hence, we expect that it would be beneficial to use such mixed-acid media in a membrane-less zinc-cerium RFB as well. Since both electrodes and half-cells are exposed to the same electrolyte in a membrane-less RFB, it is essential to first investigate the influence of such mixed electrolytes on the zinc deposition and dissolution reactions that occur at the negative electrode during the charge and discharge of a zinc-cerium RFB.

The Zn/Zn(II) half-cell reaction has been studied in methanesulfonic [6,17],

sulfuric [18,19,20,21] and chloride [21,22,23] baths. However, to the best of our knowledge, no study on this system in a mixed electrolyte has been reported. The standard rate constant reported in pure chloride solutions is 8.78×10^{-3} $\mathrm{cm\,s^{-1}}$ [24], which is about an order of magnitude higher than the value of 0.16×10^{-3} $\mathrm{cm\,s^{-1}}$ obtained in MSA-only electrolytes [25]. This reflects the beneficial role of chlorides in enhancing the kinetics of the zinc redox reaction. Based on the well-known behavior of metal deposition systems in general, we expect that the addition of chloride ions to the base MSA electrolyte will be beneficial to zinc deposition. It has been reported that the presence of chloride in zinc electrowinning baths leads to lower polarization resistance and higher charge efficiency of zinc deposition [26]. Additionally, cyclic voltammetry experiments have shown that the overpotential is reduced and the cathodic peak potential is shifted in the positive direction when zinc deposition is carried out in chloride-only baths rather than sulfate-only electrolytes [21]. Chloride ions have also improved the deposition performance of other metals and alloys such as nickel [27], copper [28], chromium [29], indium [30] and Co-Ni alloys [31]. Thus, it is reasonable to investigate the use of chloride ions to facilitate the zinc deposition process.

In terms of the effect of electrolyte composition on zinc electrodissolution, a thermometric study has shown that both chloride and sulfate tend to promote the oxidation of zinc in acidic media and should be considered as corrosive anions although it was not possible to easily differentiate between their relative strengths as corrosion promoters [32]. Although the effect of chloride on zinc dissolution in highly acidic methanesulfonate-based electrolytes has not been reported to date, halogens including chloride have been shown to increase the rate of the Zn(II)/Zn(Hg) reduction and oxidation reaction when they are added to a $NaClO_4$ base electrolyte [33], [34].

In this experimental study, we use a 3-electrode system to determine the electrolyte composition and operating conditions that optimize the kinetics of zinc electrodeposition and electrodissolution in mixed-electrolyte media with particular emphasis on methanesulfonate/chloride solutions. Carbon electrodes

have been commonly used in RFB systems due to their chemically inert nature. In some applications, the carbon electrode must be coated to avoid corrosion by corrosive ions (i.e. cerium in the case of an undivided zinc cerium RFB). Moreover, the negative electrode can be modified to inhibit undesired side reactions. For example, indium-modified graphite electrodes can be used on the negative side of the zinc-cerium RFBs to reduce hydrogen evolution [35]. In this work, we use a glassy carbon disk electrode as the working electrode. Since the ultimate aim is to determine the optimum operating conditions for a zinc-cerium RFB, we apply compositions that are typically used for this application. The undivided zinc-cerium RFBs are operated at lower acid concentrations ($\sim$ 0.2 $\mathrm{mol\,dm^{-3}}$ – 0.5 $\mathrm{mol\,dm^{-3}}$ MSA base electrolyte) [15,16], while the negative half-cell of a divided zinc-cerium RFB typically contains a higher acid concentration of $\sim$ 1 $\mathrm{mol\,dm^{-3}}$ MSA. Thus, in order to address both possible situations, we investigate Zn electrodeposition/electrodissolution in two sets of solutions containing either 0.2 $\mathrm{mol\,dm^{-3}}$ or 1 $\mathrm{mol\,dm^{-3}}$ MSA base electrolyte. In particular, the effects of temperature, acid concentration and Zn(II) concentration on the behavior of the Zn/Zn(II) system in mixed-electrolyte media are determined.

2. Experimental

For these experiments, a custom-made three-electrode water-jacketed glass cell (Adams & Chittenden Scientific Glass) was employed. The capacity of the cell is $\sim$ 200 ml and the outer cell has the dimensions of 110 mm diameter $\times$ 55 mm height. This cell was connected to a circulating bath (Neslab RTE-8) to control the electrolyte temperature throughout the experiments. All electrochemical experiments were carried out using an EPP-400 potentiostat (Princeton Applied Research). The reference electrode was a saturated glass body calomel electrode (Fisher Scientific) and the counter electrode was a graphite rod (6.15 mm diameter $\times$ 50 mm long). All electrode potentials reported herein correspond to the SCE scale. The working electrode was a glassy carbon (GC) disk of 3 mm diameter (area $\sim$ 0.071 $\mathrm{cm^2}$). The GC electrode tip has a PTFE

holder that was fitted to the EDI101 rotator and CTV speed control unit (Radiometer Analytical) for the rotating disk electrode (RDE) experiments. The GC electrode was polished manually with 0.05 µm alumina powder (Buehler) on a MicroCloth polishing pad (Buehler) for several minutes to a mirror finish prior to each experiment. The electrode was then rinsed thoroughly with ultra-pure water (resistivity $\sim$ 18 MΩ cm). It has been shown that the ferricyanide/ferrocyanide redox reaction is sensitive to the cleanliness and preparation method of GC electrodes [36]. Thus, the cleanliness of the GC electrode was assessed by carrying out a cyclic voltammetry scan first from 0.6 to 0 V *vs* SCE and then reversing back to 0.6 V at a scan rate of 100 mV s^{-1} in a solution containing 1 mmol dm^{-3} ferricyanide and 1 mol dm^{-3} KCl and measuring the separation between the cathodic and anodic potential peaks for the ferricyanide/ferrocyanide redox couple. Ideally the separation should be close to 60 mV, as expected for a 1-electron reaction. We measured the peak separation using our clean GC electrode to be 69 mV, which is close to the reported value. After each test with ferricyanide, the electrode surface was again rinsed thoroughly with water.

All solutions used for the zinc deposition/dissolution experiments were prepared with analytical grade reagents and ultra-pure water (resistivity $\sim$ 18 MΩ cm). To prevent possible interference from the oxygen reduction reaction, the solutions were purged with nitrogen gas prior to each deposition experiment for 10 minutes and the subsequent experiments were conducted under a blanket of nitrogen gas. The zinc(II) methanesulfonate solutions were prepared by dissolving the appropriate amounts of high purity zinc oxide (Zochem Inc.) in 70% methanesulfonic acid (Alfa Aesar), while sodium methanesulfonate solutions were prepared by dissolving sodium carbonate decahydrate (Alfa Aesar) in 70% methanesulfonic acid. The resulting solutions were colorless with no sign of any precipitate forming. Anhydrous zinc chloride (99% purity; Fisher Scientific) and zinc sulfate heptahydrate (98% purity; Alfa Aesar) were added to these solutions in order to introduce the chloride and sulfate ions into the mixed-electrolyte media. In order to compare the mixed-electrolyte media with

pure chloride and sulfate baths, solutions were also made with hydrochloric acid (Sigma Aldrich) and sulfuric acid (Sigma Aldrich) instead of methanesulfonic acid. Solutions that contain MSA, HCl and H_2SO_4 have a pH close to zero. In order to increase the pH of the solutions to higher values (pH 4) for the RDE experiments, 0.5 mol dm^{-3} sodium methanesulfonate, sodium chloride (EMD Millipore) and sodium sulfate (EMD Millipore) were added to the sulfonic-, chloride- and sulfate-based solutions, respectively, followed by the appropriate amounts of MSA, HCl and H_2SO_4, respectively. The kinematic viscosity of the solutions was measured using a Cannon-Fenske viscometer tube. The pH of the solutions was measured with an Orion (420A) pH meter.

The electrochemical techniques conducted included cyclic voltammetry, linear polarization and galvanostatic deposition/dissolution under unstirred conditions and linear sweep voltammetry using a rotating disk electrode. Zinc deposition onto the GC electrode was carried out galvanostatically for 30 seconds at a constant current density of 25 mA cm^{-2}, followed by zinc dissolution with the same current density. To prevent excessive oxidation of the electrode surface, zinc dissolution was halted when the potential shifted to values more positive than -0.5 versus SCE. For the morphology study, deposition onto a glassy carbon plate (Alfa Aesar) was carried out. The plate was taped with an insulating polyester tape (Cole-Parmer) to ensure that the area of the working electrode exposed to the solution was 0.5 $\times$ 0.5 cm^2. In this case, zinc deposition was done galvanostatically at a current density of 50 mA cm^{-2} for 1 minute. The images of the deposits were taken with a scanning electron microscope model Zeiss FESEM 1530.

3. Results and Discussion

Table 1 shows the compositions of the different electrolytes investigated in this study. As can be seen, MSA is the base acid in most of the samples. MSA is less corrosive than hydrochloric acid and sulfuric acid, but has comparable conductivity [37]. Moreover, only moderately high concentrations of chloride

are suitable for the electrolyte to be used in a membrane-less zinc-cerium RFB due to the possibility of chlorine gas forming in the presence of Ce(IV). Also, it has been reported that the solubility of Ce(III) in sulfate baths is considerably lower than in MSA media [9]. With these considerations, MSA is the better choice as the base electrolyte.

Table 1: Electrolyte compositions investigated in this study

Low acid concentration			
Base electrolyte ($mol\,dm^{-3}$)	ZnMSA ($mol\,dm^{-3}$)	$ZnCl_2$ ($mol\,dm^{-3}$)	$ZnSO_4$ ($mol\,dm^{-3}$)
0.2 MSA	0.7	0	0
0.2 MSA	0.5	0.2	0
0.2 MSA	0.5	0	0.2
0.2 MSA	0.3	0.4	0
0.2 MSA	0.3	0	0.4
0.2 HCl*	0	0.7	0
0.2 H_2SO_4*	0	0	0.7
High acid concentration			
1.0 MSA	1.5	0	-
1.0 MSA	1.3	0.2	-
1.0 MSA	1.2	0.3	-
1.0 HCl*	0	1.5	-

* For comparison

Since undivided zinc-cerium RFBs are usually operated at lower acid concentrations [15,16], a 0.2 $mol\,dm^{-3}$ MSA base electrolyte containing a total of 0.7 $mol\,dm^{-3}$ Zn(II) is used for one series of voltammetry experiments (Table 1). The total Zn(II) concentration is kept fixed in order to fairly compare the results obtained in the various solutions. For this series of experiments, solutions with mixed methanesulfonate/sulfate have also been prepared since it has been reported that the solubility of Ce(IV) increases in the mixed methanesulfonate/sulfate system [10] which would be beneficial for an undivided zinc-cerium RFB. On the other hand, divided zinc-cerium RFBs operate at much higher

Zn(II) concentrations (1.5 mol dm^{-3} ZnMSA in 1 mol dm^{-3} MSA [5]). Thus, 1 mol dm^{-3} MSA base electrolytes containing a total of 1.5 mol dm^{-3} Zn(II) are used for another series of voltammetry experiments (Table 1).

3.1. Effect of mixed methanesulfonate/chloride electrolyte

Figure 1 shows the cyclic voltammograms obtained in the different mixed methanesulfonate/chloride electrolytes with a total of 0.7 mol dm^{-3} Zn(II) in 0.2 mol dm^{-3} MSA (Table 1) at 25°C on a static glassy carbon electrode. The potential is swept first from -0.5 to -1.3 V *vs* SCE and then reversed back to -0.5 V at a scan rate of 20 mV s^{-1}. A nucleation loop appears during the cathodic scan obtained in each solution and is typical of that observed during metal electrodeposition. In each case, an oxidation peak during the reverse scan arises due to the anodic stripping of Zn(II) into the solution from the metal coating deposited during the previous cathodic portion of the scan.

The voltammograms clearly show that the addition of chloride ions to the electrolyte significantly increases the cathodic and anodic current densities at any particular potential during the scans and decreases the nucleation overpotential (NOP). The NOP is the difference between the nucleation potential E_{nu} (point A) at which cathodic current is first observed during the scan and the crossover potential E_{co} (point B) at which the current switches from cathodic to anodic during the reverse scan and represents the degree of polarization of the cathode [38]. As shown in Table 2, the reduction in the NOP obtained in the mixed methanesulfonate/chloride electrolytes containing a total of 0.7 mol dm^{-3} Zn(II) relative to that in the MSA-only solution reaches as high as 50 mV. The amount of zinc deposited during the cathodic portion of each scan can be determined by measurement of the anodic charge (Q_{an}) during the reverse scan. Analysis of the CVs in Figure 1 shows that the amount of zinc deposited has increased by 57% and 129% when 0.2 and 0.4 mol dm^{-3} chloride ion, respectively, replace MSA in the electrolyte (Table 2). Note that the total Zn(II) concentration is kept fixed at 0.7 mol dm^{-3} in these solutions so that these differences can be attributed to the amount of chloride present.

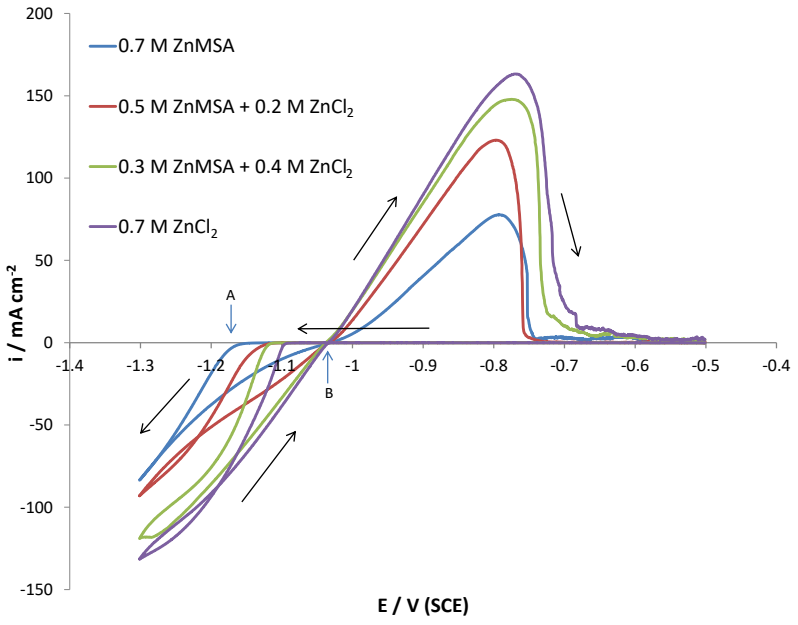

Figure 1: Cyclic voltammograms on a glassy carbon electrode (~ 0.071 cm^2) in different mixed methanesulfonate/chloride media with 0.2 mol dm^{-3} MSA base electrolyte at 25°C and a scan rate of 20 mV s^{-1}.

A similar trend is observed in the cyclic voltammograms in Figure 2 obtained in the different mixed methanesulfonate/chloride electrolytes listed in Table 1 which contain a total of 1.5 mol dm^{-3} Zn(II) in 1 mol dm^{-3} MSA (typical composition of the negative half-cell in divided RFBs). As shown in Table 2, the NOP decreases by 90 mV when 0.3 mol dm^{-3} chloride ion substitutes for MSA in the electrolyte. Furthermore, Q_{an} increases by 113% relative to the value obtained in the 1.5 mol dm^{-3} ZnMSA solution when MSA is replaced by 0.2 mol dm^{-3} chloride and by 179% when it is replaced by 0.3 mol dm^{-3} chloride.

Due to the highly acidic environment of the studied electrolytes, hydrogen evolution (HER) also accompanies zinc deposition during cathodic polarization. In order to determine if the higher cathodic current density obtained in the mixed methanesulfonate/chloride media is due to zinc deposition or hydrogen

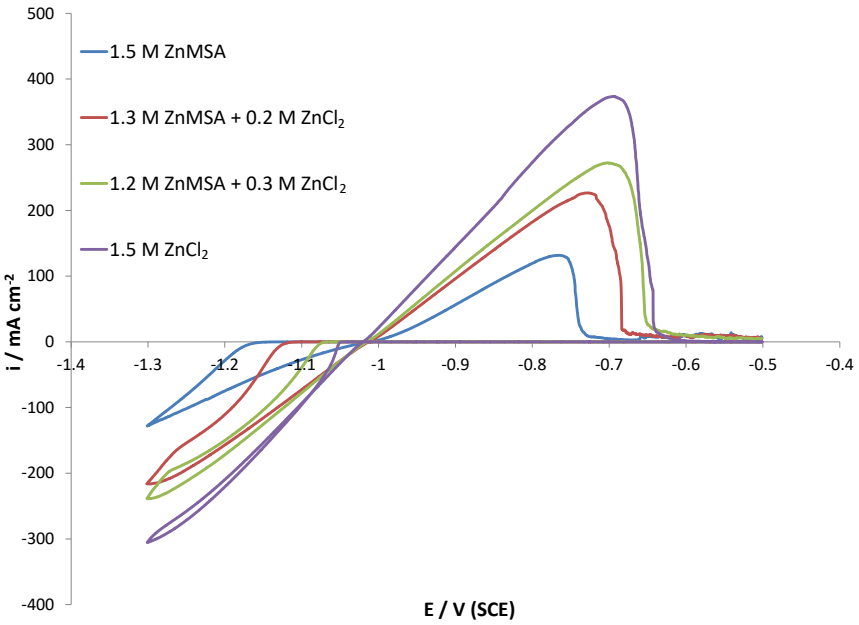

Figure 2: Cyclic voltammograms on a glassy carbon electrode (~ 0.071 cm^2) in different mixed methanesulfonate/chloride media with 1.0 mol dm^{-3} MSA base electrolyte at 25°C and a scan rate of 20 mV s^{-1}.

evolution, the charge efficiency (CE) over each of the voltammograms has been determined and included in Table 2. The charge efficiency is calculated as the ratio of the charge passed during the anodic portion of the scan to that obtained during the cathodic portion. Table 2 shows that higher charge efficiency is achieved in the mixed-electrolyte media than in the MSA-only electrolyte. Thus, the mixed methanesulfonate/chloride electrolyte does not appear to promote the HER and the higher current densities observed in the presence of chloride can be attributed to an increase in the zinc deposition/dissolution rate.

Although a higher concentration of chloride ions in the mixed-electrolyte media improves the zinc half-cell reaction kinetics, it would be preferable to maintain the Cl^- concentration at lower levels in a membrane-less zinc-cerium RFB due to the concern that it could be oxidized by Ce(IV) also present in the electrolyte. Thus, based on the results of this section, a composition of

Table 2: Effect of electrolyte composition on E_{nu}, NOP, Q_{an} and CE of zinc deposition in mixed electrolyte solutions compared to pure methanesulfonate, chloride and sulfate solutions.

Composition (mol dm^{-3})	E_{nu} (V)	-NOP (mV)	Q_{an} (mA s)	CE (%)
0.2 mol dm^{-3} MSA base electrolyte				
0.7 ZnMSA	-1.15	120	42.9	85
0.5 ZnMSA+ 0.2 $ZnCl_2$	-1.11	80	67.4	93
0.3 ZnMSA + 0.4 $ZnCl_2$	-1.11	70	98.4	89
0.7 $ZnCl_2$	-1.09	60	114.2	88
0.5 ZnMSA+ 0.2 $ZnSO_4$	-1.17	130	27.1	88
0.3 ZnMSA+ 0.4 $ZnSO_4$	-1.17	130	25.2	85
0.7 $ZnSO_4$	-1.18	130	31.3	89
1.0 mol dm^{-3} MSA base electrolyte				
1.5 ZnMSA	-1.15	140	73.4	83
1.3 ZnMSA+ 0.2 $ZnCl_2$	-1.11	100	156.1	94
1.2 ZnMSA + 0.3 $ZnCl_2$	-1.07	50	204.8	90
1.5 $ZnCl_2$	-1.05	30	277.7	87

0.5 mol dm^{-3} ZnMSA/0.2 mol dm^{-3} $ZnCl_2$ in 0.2 mol dm^{-3} MSA is chosen for subsequent analysis as an electrolyte in an undivided RFB (see section 3.4). For a divided zinc-cerium RFB, higher chloride concentrations can be used with the MSA base electrolyte. Thus, for this application, we will focus on the composition of 1.2 mol dm^{-3} ZnMSA/0.3 mol dm^{-3} $ZnCl_2$ in 1 mol dm^{-3} MSA. Although not included here, experiments have also been conducted in solutions containing more $ZnCl_2$ (i.e., 1.0 mol dm^{-3} ZnMSA/0.5 mol dm^{-3} $ZnCl_2$ in 1 mol dm^{-3} MSA), but little further change in the electrode response from that obtained in 1.2 mol dm^{-3} ZnMSA/0.3 mol dm^{-3}) $ZnCl_2$ in 1 mol dm^{-3} MSA was observed. Thus, no further experiments in electrolytes containing more than 0.3 mol dm^{-3} $ZnCl_2$ have been conducted.

3.2. Effect of mixed methanesulfonate/sulfate electrolyte

Figure 3 shows cyclic voltammograms of the Zn/Zn(II) system in different mixed methanesulfonate/sulfate electrolytes and the corresponding pure electrolytes containing a total dissolved Zn(II) concentration of 0.7 mol dm^{-3} in

0.2 mol dm^{-3} MSA (Table 1). As Table 2 shows, the presence of sulfate ions has a different effect from that of chloride by leading to a slight increase in E_{nu} ($\sim$ 20 mV), reflecting of a larger overpotential and more difficult onset of zinc electrodeposition in mixed methanesulfonate/sulfate electrolyte compared to the pure ZnMSA electrolyte. Although the charge efficiencies are comparable in both pure and mixed electrolytes, the current density throughout the cathodic portion of the scan and the anodic charge reflecting the amount of zinc deposited are lower in the sulfate-containing solutions. Thus, although a mixed methanesulfonate/sulfate electrolyte would have some benefits in an undivided zinc/cerium RFB since it enhances the Ce(IV) solubility [10], our results show that the kinetics of the Zn/Zn(II) redox reaction will suffer.

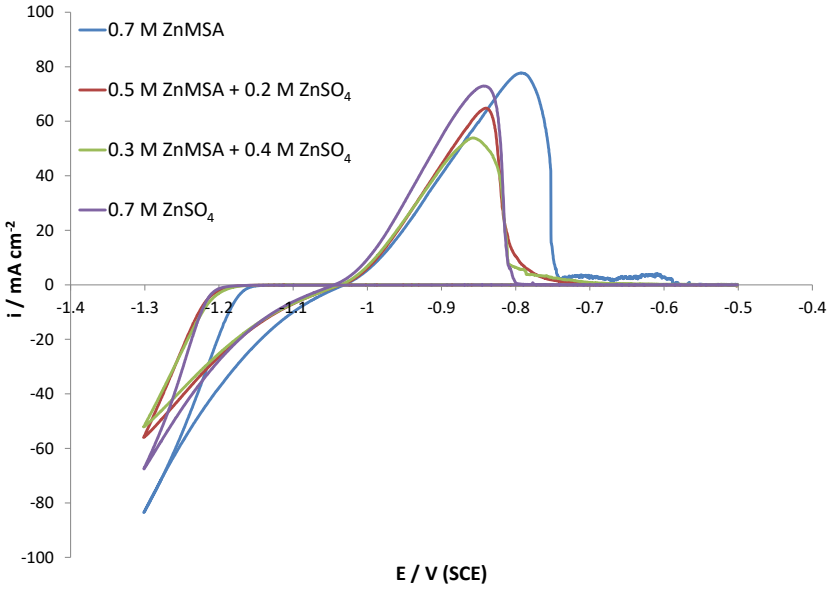

Figure 3: Cyclic voltammograms on a glassy carbon electrode ($\sim$ 0.071 cm^2) in different mixed methanesulfonate/sulfate media with 0.2 mol dm^{-3} MSA base electrolyte at 25°C and a scan rate of 20 mV s^{-1}.

The CVs in these previous two sections clearly show that the addition of chloride ions to the MSA base electrolyte leads to larger cathodic and anodic

current densities and more zinc deposition compared to that obtained in the pure MSA and sulfate-containing electrolytes. Also, the effect of the anions on the overpotential for zinc deposition on glassy carbon electrode increases in the following order: $Cl^- < CH_3SO_3^- < SO_4^-$. As previously mentioned, chloride ions have been shown to enhance the electrodeposition of other metals as well. One proposed mechanism for this effect is the bridging effect of chloride ions [30,39]. In this mechanism, the chloride ions adsorb on the electrode substrate and facilitate the electron transfer between the metal cations and the electrode by forming bridges between them [30].

Another important factor is the strength of the interaction between Zn(II) and the various ligands present which must be overcome in order to discharge and deposit the metal. Consequently, the more stable a zinc ion-pair or complex is, the slower should be the rate of zinc nucleation and deposition. One measure of the strength of such an interaction is the magnitude of the stability constant for its formation. The stability constant for the formation of the $ZnCl^+$ complex at zero ionic strength is $10^{0.96}$ [40]. On the other hand, the stability constant for the formation of $ZnSO_4$ complex at zero ionic strength is $10^{2.38}$ [40]. Based on this criterion, it should be easier to discharge Zn(II) and deposit metal in the former than the latter electrolyte. This can explain the lower overpotential for Zn(II) reduction in a mixed methanesulfonate/chloride bath compared to a mixed methanesulfonate/sulfate electrolyte. No data were found in the literature for the stability constant of zinc methanesulfonate complexes. However, it has been reported that methanesulfonate ions are stronger complexing agents than chloride for other metals such as lead and cadmium [41]. Additionally, a previous study on nickel deposition has shown that the overpotential for Ni(II) reduction increases in the sequence $ClO_4^- < CH_3SO_3^- < SO_4^-$, which leads to the expectation that nickel-methanesulfonate complexes are less thermodynamically favored than nickel-sulfate complexes and more than those containing chloride [42]. In this study, we have found a similar trend in the overpotential for Zn(II) reduction and thus propose that the stability of zinc-methanesulfonate complexes is also higher than that of zinc-chloride complexes, leading to the

mixed methanesulfonate/chloride bath being the most favorable electrolyte for deposition.

3.3. Determination of exchange current density

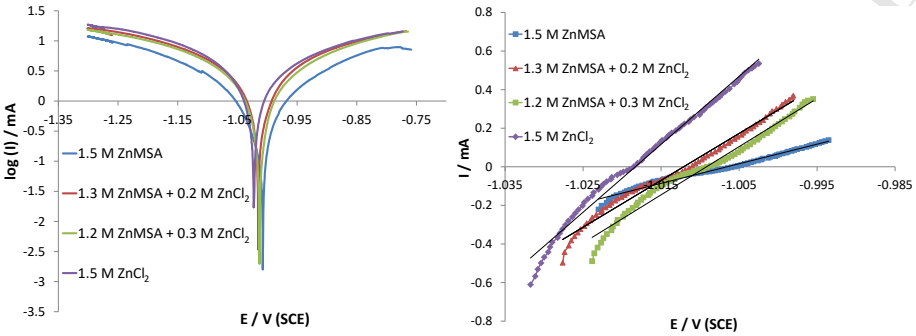

(a) (b)

Figure 4: (a) Semi-log plot of current versus potential on a glassy carbon electrode (~ 0.071 cm^2) immersed in different mixed methanesulfonate/chloride media obtained at a scan rate of 2 $mV\,s^{-1}$. (b) Linear polarization measurements for zinc on a glassy carbon electrode obtained at a scan rate of 0.167 $mV\,s^{-1}$.

Our results in Table 2 suggest that the addition of chloride enhances the kinetics of the zinc redox reaction. Thus, we have conducted polarization experiments to find the change in the values of exchange current densities upon addition of chloride to the solution. Figure 4a is obtained by scanning the potential at a sweep rate of 2 $mV\,s^{-1}$ up to 0.250 V in both directions from the open circuit potential for each electrolyte shown in Table 3. The Butler-Volmer equation (Eqn (1)) has been fitted to the experimental data to obtain the exchange current density (i_0), β_a and β_c. A non-linear least-square method that makes use of the trust region reflective algorithm (TRF) has been used to do this fitting.

$$i = i_0 \left(\exp(\frac{2.3(E - E_{ocp})}{\beta_a}) - \exp(-\frac{2.3(E - E_{ocp})}{\beta_c}) \right) \quad (1)$$

As Table 3 shows, the exchange current density increases from 11.3×10^{-3} A cm^{-2} to 21.7×10^{-3} A cm^{-2} upon addition of 0.2 mol dm^{-3} $ZnCl_2$ and rises to 24.0×10^{-3} A cm^{-2} when 0.3 mol dm^{-3} $ZnCl_2$ is added. The highest exchange current density was found for the pure $ZnCl_2$ solution. These values are in the same range (10^{-3} A cm^{-2}) as the reported values for zinc redox reaction in pure chloride and MSA electrolytes [43,44]. It should be noted that as Table 3 shows, the β_c and β_a extracted from Figure 4a are all larger than the expected value for a two-electron transfer (60 mV decade^{-1}). However, they are in agreement with the values reported in previous studies on zinc deposition and dissolution reaction in pure MSA solutions [45].

For the linear polarization technique, a potential sweep rate of 0.117 mV s^{-1} was used and the potentials were limited to 0.010 V from the open circuit potential. In this range of overpotential, current changes linearly with voltage (Figure 4b). Similar to the results found from fitting the Butler-Volmer equation to the experimental data, the exchange current densities increase as the chloride concentration is raised. The difference between the values obtained by these two methods has also been reported in a previous study on zinc redox reaction in pure MSA electrolyte [45] and is attributed to the occurrence of hydrogen evolution reaction particularly at higher overpotentials.

Table 3: Open circuit potential (E_{ocp}), $-\beta_c$ and β_a along with the exchange current density (i_0) calculated from fitting the Butler-Volmer equation to experimental data and use of the linear polarization method.

Compositon (mol dm^{-3})	Fitting of Butler-Volmer Equation				Linear polarization
	E_{ocp} (V)	$-\beta_c$ (mV decade^{-1})	β_a (mV decade^{-1})	i_0 mA cm^{-2}	i_0 mA cm^{-2}
1.5 ZnMSA	-1.008	177	170	11.3	5.4
1.3 ZnMSA + 0.2 $ZnCl_2$	-1.011	170	170	21.7	12.7
1.2 ZnMSA + 0.3 $ZnCl_2$	-1.014	200	200	24.0	15.2
1.5 $ZnCl_2$	-1.023	181	200	27.0	21.9

3.4. Determination of diffusion coefficients for Zn(II)

In order to study the possible effect of chloride and sulfate ions on the transport properties of Zn(II), we conducted a series of linear sweep voltammetry experiments on a rotating GC electrode in various Zn(II)-containing solutions over the potential range where zinc deposition occurs. As mentioned previously, zinc deposition is accompanied by HER in all the electrolytes considered so far in this study due to their acidic conditions. This greatly complicates the accurate determination of the diffusion coefficient of Zn(II) using the Levich equation since the limiting current plateaus for its reduction do not clearly appear in the linear sweep voltammograms obtained in these solutions. Consequently, we have chosen to measure the Zn(II) diffusion coefficients in electrolytes that contain lower Zn(II) concentrations and are less acidic to ensure that it is possible for the measured current to be controlled by diffusion of Zn(II) alone. Table 4 shows the composition of the electrolytes used for estimation of the diffusion coefficients. The pure MSA and mixed electrolyte solutions are adjusted to pH 4 by adding 0.5 $\mathrm{mol\,dm^{-3}}$ NaMSA and the appropriate amount of MSA. Solutions with pure chloride and sulfate ions have also been characterized for comparison. 0.5 $\mathrm{mol\,dm^{-3}}$ NaCl or Na_2SO_4 are added to these solutions and the pH is adjusted to 4 using the appropriate amount of HCl or H_2SO_4.

Figure 5a shows the cyclic voltammograms obtained in the different mixed methanesulfonate/chloride electrolytes containing a total of 0.02 $\mathrm{mol\,dm^{-3}}$ Zn(II) (Table 4) at 25°C on a static glassy carbon electrode. In these experiments, the potential is swept first from -0.8 to -1.4 V *vs* SCE and then reversed back to -0.8 V at a scan rate of 20 $\mathrm{mV\,s^{-1}}$. Similar to that observed previously in the more concentrated solutions, the addition of chloride shifts the E_{nu} to more positive values and increases the current density and amount of zinc deposited. As reported previously [6], the limiting current density i_L is an important factor in the charge/discharge of RFBs. Operation at current densities higher than i_L leads to excessive hydrogen evolution and hence a lower charge efficiency when the battery is being re-charged. Figure 5b shows the electrode responses obtained at 1600 rpm for the same compositions shown in Figure 5a. As can

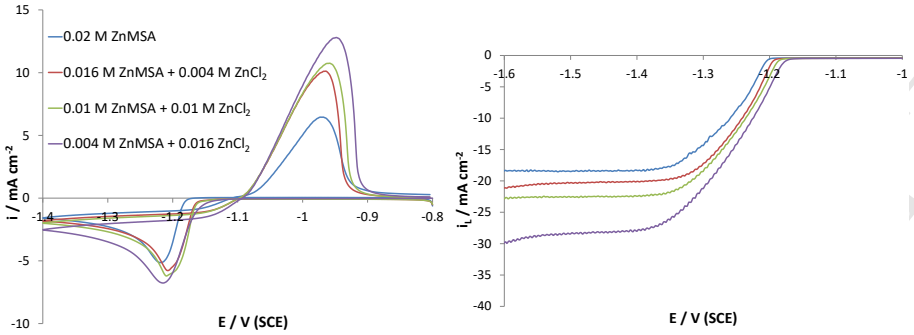

(a) (b)

Figure 5: (a) Cyclic voltammograms on a glassy carbon electrode ($\sim$ 0.071 cm^2) immersed in different mixed methanesulfonate/chloride media at 25°C obtained at a scan rate of 20 $mV\,s^{-1}$. (b) Comparison of linear sweep voltammograms for RDE rotating at 1600 rpm for the same compositions shown in Figure 5a. Scan rate = 20 $mV\,s^{-1}$.

be seen, these plots show that the limiting current density for Zn(II) reduction is increased significantly by the presence of chloride (e.g., an increase from $\sim$ -18 $mA\,cm^{-2}$ to $\sim$ -29 $mA\,cm^{-2}$ as the $ZnCl_2$ concentration is raised from 0 to 0.016 $mol\,dm^{-3}$) despite the fact that the total amount of Zn(II) in solution remains unchanged. A similar trend is observed at the other rotation speeds.

Linear sweep experiments over the potential range from -1.0 V to -1.9 V *vs* SCE at a scan rate of 20 $mV\,s^{-1}$ on an RDE operating at rotation speeds of 400, 900, 1600, 2500 and 3600 rpm have been conducted for each composition given in Table 4. Figure 6a shows an example of the set of linear sweep voltammograms obtained in one of the solutions (0.01 $mol\,dm^{-3}$ ZnMSA/0.01 $mol\,dm^{-3}$ $ZnCl_2$ in 0.5 $mol\,dm^{-3}$ NaMSA) at pH 4. The current density for the mass transport-limited reaction of an electroactive species at a rotating disk electrode is described by the Levich equation [46]

$$i_L = 0.620nFD^{2/3}\omega^{1/2}v^{-1/6}c \qquad (2)$$

where n is the number of transferred electrons (2 in this case), F is the Faraday constant, D is the diffusion coefficient, ω is the rotation speed expressed in

rad s^{-1}, v is the kinematic viscosity and c is the concentration of the electroactive species. Figure 6b shows a plot of i_L versus $w^{1/2}$ according to the Levich equation for the solution considered in Figure 6a. As predicted by the Levich equation, the plot is linear and passes through the origin. Although not included here, similar results are obtained for the other solutions. Table 4 shows the diffusion coefficients obtained from the slope of the best straight line plot for various electrolytes. Also included in the table are the corresponding kinematic viscosities measured directly in our study. The dimensionless Schmidt number which is the ratio of the dynamic viscosity of the electrolyte to the diffusion coefficient is also included in this table. This number is important for characterizing the flow conditions and is relevant to the design of redox flow batteries. The diffusion coefficient of zinc in pure methanesulfonate, sulfate and chloride solutions is found to be 4.6×10^{-6} $cm^2\,s^{-1}$, 4.4×10^{-6} $cm^2\,s^{-1}$, 8.6×10^{-6} $cm^2\,s^{-1}$, respectively. The values obtained in the sulfate- and chloride-only solutions are in good agreement with those reported previously [18,22]. In a previous study [10] the diffusion coefficient of Zn(II) in a pure methanesulfonate solution was found to have a somewhat higher value of 7.5×10^{-6} $cm^2\,s^{-1}$ than that reported here although it should be noted that this earlier measurement was conducted in a solution with a different concentration (0.01 mol dm^{-3} ZnMSA in 0.5 mol dm^{-3} NaMSA). Also, in this earlier study, the kinematic viscosity of the electrolyte was not measured and instead a value from the literature was assumed for the purpose of estimating diffusion coefficient.

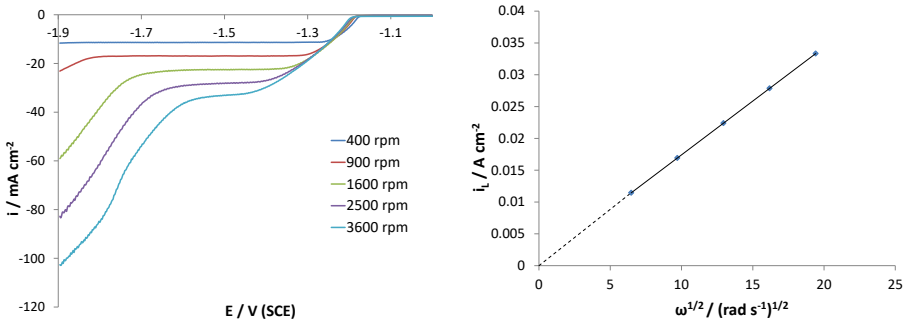

(a) (b)

Figure 6: (a) Linear sweep voltammograms for Zn(II) reduction on a glassy carbon electrode ($\sim$ 0.071 cm^2) obtained at a scan rate of 20 $mV\,s^{-1}$ and different rotation speeds in 0.01 $mol\,dm^{-3}$ ZnMSA/0.01 $mol\,dm^{-3}$ $ZnCl_2$ and 0.5 $mol\,dm^{-3}$ NaMSA at pH 4. (b) Plot of limiting current density versus $\omega^{1/2}$ according to the Levich equation obtained in the same solution.

Table 4: Kinematic viscosity, diffusion coefficient and Schmidt number measured in various mixed electrolytes.

Composition ($mol\,dm^{-3}$)	Kinematic viscosity (10^{-2} $cm^2\,s^{-1}$)	Diffusion coefficient (10^{-6} $cm^2\,s^{-1}$)	Schmidt number
0.02 ZnMSA	1.064	4.6	0.23
0.016 ZnMSA + 0.004 $ZnCl_2$	1.092	5.3	0.21
0.01 ZnMSA + 0.01 $ZnCl_2$	1.076	6.0	0.18
0.004 ZnMSA + 0.016 $ZnCl_2$	1.088	8.3	0.13
0.02 $ZnCl_2$	1.012	8.5	0.12
0.016 ZnMSA + 0.004 $ZnSO_4$	1.052	4.4	0.24
0.01 ZnMSA + 0.01 $ZnSO_4$	1.064	5.1	0.21
0.004 ZnMSA + 0.016 $ZnSO_4$	1.052	5.7	0.18
0.02 $ZnSO_4$	1.360	4.4	0.31

** pH of all solutions adjusted to 4 through additions of 0.5 $mol\,dm^{-3}$ NaMSA to the methanesulfonate solutions and 0.5 $mol\,dm^{-3}$ NaCl or Na_2SO_4 to the chloride- or sulfate-only solutions.

435 The results in Table 4 show that as more ZnMSA is replaced with $ZnCl_2$
436 in the electrolyte, the diffusion coefficient increases and approaches the value

obtained in a solution containing $ZnCl_2$ alone. On the other hand, the diffusion coefficients in the mixed methanesulfonate/sulfate media differ only slightly from the values observed in the sulfate-only or methanesulfonate-only electrolytes.

3.5. Effect of operating parameters in mixed methanesulfonate/chloride electrolyte

3.5.1. Effect of temperature

Temperature is one of the important operating variables for redox flow batteries. Whereas the proposed undivided zinc-cerium RFB has been operated at room temperature [15], higher temperatures (40°C-60°C) have been used for the divided zinc-cerium RFBs [5]. Thus, the effect of temperature on the Zn/Zn(II) system in mixed methanesulfonate/chloride media is compared to that in the MSA-only electrolyte for compositions used on the zinc negative half-cell side of a divided zinc-cerium RFB.

Figure 7 shows the cyclic voltammograms obtained in solutions containing 1.2 $\mathrm{mol\,dm^{-3}}$ ZnMSA/0.3 $\mathrm{mol\,dm^{-3}}$ $ZnCl_2$ in 1 $\mathrm{mol\,dm^{-3}}$ MSA compared to those obtained in the MSA-only electrolyte (1.5 $\mathrm{mol\,dm^{-3}}$ ZnMSA in 1 $\mathrm{mol\,dm^{-3}}$ MSA) at 25, 35 and 45°C. The values of E_{nu}, NOP , I_{ac} and Q_{an} determined from these plots for both electrolytes at the three temperatures are summarized in Table 5. These data show that an increase in temperature leads to a positive shift of E_{nu} in both electrolytes, but has much less effect in the mixed methanesulfonate/chloride solution. An increase of E_{nu} is expected from both thermodynamic and kinetic points of view. The electrode potential for Zn/Zn(II) increases with temperature according to the Nernst equation, while the rate of formation of metal clusters large enough to ensure spontaneous growth should also rise with temperature as given in classical nucleation theory and the Volmer-Weber equation [47]. The data in Table 6 indicate that an increase in temperature causes the amount of zinc deposited during the scan to rise and NOP to decline in both electrolytes. However, they also reveal that the rise in E_{nu} and the amount of zinc deposited during the cathodic scan are significantly

higher and NOP is always smaller in the mixed system than in the MSA-only electrolyte at each temperature. At 45 °C, the amount of deposited zinc is 50% higher and the NOP is 86% lower when the mixed electrolyte is used than when MSA-only media are used. Although the NOP tends to decrease in magnitude with temperature, the value for the pure MSA electrolyte at 45°C is 93 mV, which is still higher than the value of 50 mV in the methanesulfonate/chloride electrolyte. This highlights the important role that chloride plays in facilitating zinc deposition. In fact, the improved kinetics achieved at 45°C in the pure MSA electrolyte is already observed in the methanesulfonate/chloride solution at room temperature.

To accurately determine the effect of temperature on the charge efficiency of Zn deposition, we also have conducted experiments in which the GC electrode immersed in the solutions of interest is galvanostatically polarized at 25 $\mathrm{mA\,cm^{-2}}$ first in the cathodic direction for 30 s and then with the same magnitude of current in the anodic direction. Figure 8 shows the resulting response of the electrode potential over this time obtained in the mixed and the MSA-only electrolytes at the three temperatures, while Table 6 summarizes the corresponding data for these experiments. The transient curves for both electrolytes show that the electrode is immediately depolarized at the onset of the cathodic polarization until a plateau is reached. This is not surprising given that the nucleation overpotential for zinc deposition should decrease as the zinc deposit begins to build on the GC substrate and is consistent with the features of the cyclic voltammograms shown in Figure 7 and Table 5. When the polarity is reversed and anodic current is applied, the response of the system is extremely rapid and a plateau is reached almost immediately in both electrolytes regardless of the temperature. This continues for $\sim$ 25–30 s of anodic polarization until all of the zinc metal deposited during cathodic polarization has been stripped, at which point the potential increases very sharply in the positive direction and the experiment is terminated. The curves in Figure 8 clearly show that temperature has a much smaller effect on the electrode response obtained in the mixed electrolyte than in the MSA-only electrolyte, which is consistent

with the effects on E_{nu} and NOP observed in the CV scans in Figure 7 and listed in Table 5. The curves in Figure 8 are relevant to battery applications in that they give the response of the negative Zn electrode that might be expected during a short charge/discharge cycle of a system operating at a given current density. Comparison of the curves reveals a number of benefits of using the mixed methanesulfonate/chloride electrolyte rather than the pure MSA electrolyte. The electrode potential reaches a plateau level where the rate of growth or re-dissolution of zinc is constant almost immediately during both the cathodic and anodic (charge and discharge) portions of the cycle at the three temperatures. On the other hand, the electrode potential never levels off to a constant value by the end of the 30–s duration of cathodic polarization in the MSA-only solution at any temperature. Once the polarity of the current is reversed in the anodic direction, the polarization of the electrode continues to gradually rise until the Zn deposit has completely dissolved from the electrode when carried out in the MSA-only electrolyte, whereas the electrode is able to maintain an almost constant potential until the Zn deposit has deposit has been removed in the case of the mixed electrolyte.

The operation of a rechargeable battery is most efficient when the polarization of both electrodes is as low as possible during both charge and discharge. Thus, it is desirable for the electrode potential to be as positive as possible during charge when Zn(II) reduction occurs and as negative as possible during discharge when Zn oxidation occurs. The result will be the smallest change in the electrode potential during the course of a complete charge/discharge cycle. When viewed this way, a comparison of the transient curves in Figure 8 clearly shows that with the exception of cathodic polarization at 45°C better performance is achieved in the mixed electrolyte than the pure MSA system.

Since the magnitude of the applied current is the same during both stages of these experiments, the charge efficiency for Zn deposition can simply be obtained from the data in Figure 8 from the ratio of the elapsed time required to completely strip the Zn deposit from the substrate during the anodic polarization to the period allowed for cathodic polarization (30 s in this case). The

sharp rise in the electrode potential observed when the Zn deposit has been removed makes the determination of the charge efficiency from these plots very straightforward. Although the solution conductivity and voltage efficiency both increase as temperature is raised, the charge efficiency for Zn deposition in pure MSA electrolyte has been previously shown to decrease due to the higher rate of the HER [6]. The effect of temperature in the case of mixed electrolytes has not previously been reported. The results in Table 6 not only confirm that temperature has a similar effect in the MSA-only electrolyte investigated in our study but that this effect extends to the mixed electrolyte as well. Thus, the larger cathodic current density observed during the scans in Figure 7 as the temperature is raised in both solutions is due to the higher rates of both zinc deposition and hydrogen evolution.

Nevertheless, for the most part, our results clearly show the enhanced performance of the Zn/Zn(II) reaction in mixed-electrolyte media in terms of higher voltage and charge efficiency compared to that achieved in MSA-only electrolyte at each temperature, which leads to a significantly larger energy efficiency. Even with the decrease in the charge efficiency with temperature due to the higher rate of the HER, the energy efficiency at 45°C in the mixed media is still greater than the energy efficiency achieved at room temperature in the pure MSA electrolyte. This observation is particularly important for divided zinc-cerium RFBs that are operated at higher temperatures to enhance the kinetics of the Ce(III)/Ce(IV) reaction. By using the mixed methanesulfonate/chloride electrolyte, the Zn/Zn(II) half-cell performance at 45°C is superior in terms of E_{nu}, NOP, voltage and charge efficiency to that achieved in pure MSA electrolytes at room temperature.

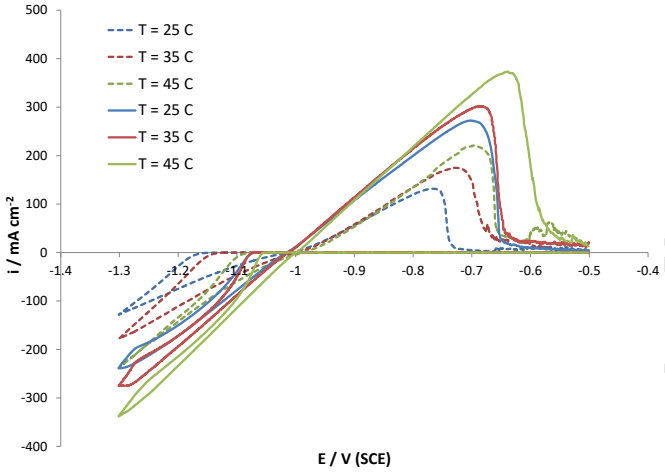

Figure 7: Cyclic voltammograms obtained on a glassy carbon electrode ($\sim$ 0.071 cm^2) in mixed methanesulfonate/chloride media (solid line) and MSA-only electrolyte (dashed line) at three different temperatures.

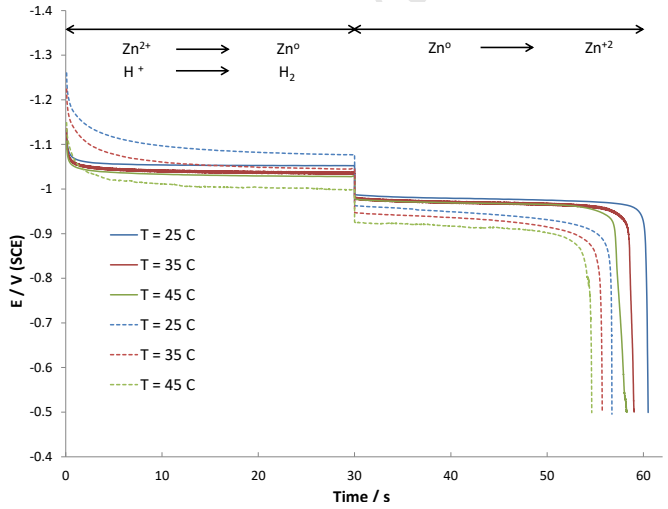

Figure 8: Variation of electrode potential with time during galvanostatic cathodic and anodic polarization of glassy carbon electrode ($\sim$ 0.071 cm^2) at 25 mA cm^{-2} in mixed methanesulfonate/chloride media (solid line) and MSA-only electrolyte (dashed line) at three different temperatures.

Table 5: Effect of temperature, MSA and zinc concentration on E_{nu}, NOP, I_{ac} and Q_{an} of zinc deposition in mixed methanesulfonate/chloride and MSA-only electrolytes. The corresponding figures and compositions for each temperature, MSA and zinc concentration are explained in sections 3.4.1, 3.4.2 and 3.4.3, respectively.

Operating parameter	E_{nu} (V)		-NOP (mV)		I_{ac} (mA cm^{-2})		Q_{an} (mA s)	
	MSA -only	Mixed electrolyte	MSA -only	Mixed electrolyte	MSA -only	Mixed electrolyte	MSA -only	Mixed electrolyte
Temperature (°C)								
25	-1.15	-1.07	140	50	131.6	272.4	73.4	204.8
35	-1.12	-1.07	122	50	174.8	301.9	111.9	230.0
45	-1.08	-1.05	93	50	220.7	373.2	152.9	309.4
MSA concentration (mol dm^{-3})								
0.2	-1.15	-1.11	120	80	77.7	123.0	42.9	67.4
0.5	-1.15	-1.12	130	80	113.7	147.0	61.1	85.0
1.0	-1.16	-1.14	150	90	125.1	208.8	64.9	90.0
Zinc concentration (mol dm^{-3})								
0.7	-1.15	-1.11	120	80	77.7	123.0	42.9	67.4
1.0	-1.14	-1.10	120	70	98.0	158.6	57.9	118.7
1.5	-1.13	-1.06	120	50	118.8	213.1	74.5	174.7

Table 6: Half-cell efficiencies of zinc deposition and dissolution of zinc in mixed MSA/chloride electrolyte and MSA-only electrolytes. The corresponding figures and compositions for each temperature, MSA, zinc concentration and current density are explained in sections 3.4.1, 3.4.2, 3.4.3 and 3.4.4 respectively.

Operating parameter	VE%		CE%		EE%	
	MSA -only	Mixed	MSA -only	Mixed	MSA -only	Mixed
Temperature (°C)						
25	87.7	92.6	86.0	97.3	75.4	90.1
35	89.2	93.0	82.3	94.3	73.5	87.7
45	91.2	93.9	77.3	86.9	70.6	80.6
MSA concentration ($\mathrm{mol\,dm^{-3}}$)						
0.2	81.1	90.9	77.0	95.0	62.4	86.4
0.5	82.9	90.6	76.0	91.7	63.0	83.5
1.0	83.9	93.6	71.3	88.7	59.8	83.0
Zinc concentration ($\mathrm{mol\,dm^{-3}}$)						
0.7	81.1	90.9	77.0	95.0	62.4	86.4
1.0	84.6	91.1	82.3	96.7	69.6	88.1
1.5	86.2	92.0	87.3	97.7	75.3	89.9
Current density ($\mathrm{mA\,cm^{-2}}$)						
5	95.5	97.1	80.0	87.7	76.4	83.1
25	87.7	92.6	86.0	97.3	75.4	90.1
35	84.5	91.0	86.7	92.7	73.2	84.3
45	80.4	87.3	85.0	93.7	68.3	81.8
55	77.6	86.7	84.3	92.3	65.4	80.9

3.5.2. Effect of methanesulfonic acid concentration

Cyclic voltammograms showing the effect of the addition of different amounts of methanesulfonic acid to a mixed methanesulfonic acid/chloride solution (0.5 $\mathrm{mol\,dm^{-3}}$ ZnMSA/0.2 $\mathrm{mol\,dm^{-3}}$ $ZnCl_2$) and to a pure MSA electrolyte (0.7 $\mathrm{mol\,dm^{-3}}$ ZnMSA) are presented in Figure 9. The corresponding data obtained from these plots are given in Table 5. The data show that the nucleation potential is largely independent of the MSA concentration and shifts only slightly in the negative direction as the MSA concentration is increased. The NOP

is affected more strongly, particularly in the MSA-only solution where it rises from 120 mV to 150 mV as the MSA level is increased from 0.2 mol dm^{-3} to 1.0 mol dm^{-3}. As can be seen, the cathodic current density and amount of zinc deposited during the scans increase in both electrolytes (pure and mixed) when the concentration of the base MSA electrolyte is raised. However, these values always remain higher for the case of the mixed electrolyte. In addition, the onset potential for zinc deposition is more positive and the NOP is significantly lower in the mixed electrolyte than in the MSA-only system.

Figure 10 shows the effect of MSA concentration on the electrode potential during the course of galvanostatic cathodic and anodic polarization of the GC electrode at 25 mA cm^{-2} in the mixed and pure MSA electrolytes, while Table 6 presents the voltage, charge and energy efficiencies obtained from these experiments. A comparison of these transients shows the clear superiority of the system performance when the mixed electrolyte is used in terms of the lower extent of polarization required to sustain the applied current during both the cathodic and anodic stages, faster attainment of plateau and charge efficiency of Zn deposition.

When the effect of MSA level in each electrolyte is considered, these data reveal that a rise in its concentration leads to more metal deposition, but favors the HER even more. This effect is perfectly understandable given that MSA is the source of H^+ ions. It should be noted that although the charge efficiency decreases as the MSA concentration increases in both solutions, the charge efficiency in the mixed methanesulfonate/chloride media remains higher than in the MSA-only electrolyte at each MSA concentration. Furthermore, although the energy efficiency of zinc deposition decreases with increasing MSA concentrations due to reduction in the charge efficiency, the energy efficiency in the mixed media containing 1.0 mol dm^{-3} MSA is significantly higher than that in pure MSA electrolyte with 0.2 mol dm^{-3} base MSA. Thus, by employing the mixed electrolyte system, it is possible to operate the cell over a wider range of MSA concentrations without the Zn/Zn(II) reaction being negatively affected. Again, this advantage of the mixed electrolyte is particularly important for an undivi-

ded zinc-cerium RFB where high MSA concentrations are required to dissolve the Ce(IV). It has been reported that the optimum composition from the point of view of the solubility of cerium species is approximately 0.8 mol dm^{-3} Ce(III) ion in 4.0 mol dm^{-3} MSA [7]. However, at this high MSA concentration, the HER becomes dominant on the zinc side. Thus, for an undivided zinc-cerium RFB, a compromise must be made between a lower hydrogen evolution rate at the zinc side and higher solubility of cerium in the electrolyte. This normally requires that the battery be operated at low MSA concentrations and consequently only at a low Ce(III) concentration ($\sim$ 0.2 mol dm^{-3}) [15]. This leads to a low energy density of 11 W h L^{-1} for an undivided system. Hence, it would be beneficial to achieve higher charge efficiencies for zinc electrodeposition when the solution contains a higher MSA concentration and the battery can produce a higher energy density. As shown in this study, this is possible by using a mixed methanesulfonate/chloride electrolyte, which enables the charge and voltage efficiency for zinc deposition achieved in the presence of 1.0 mol dm^{-3} MSA to be better to that achieved when only 0.2 mol dm^{-3} MSA has been added.

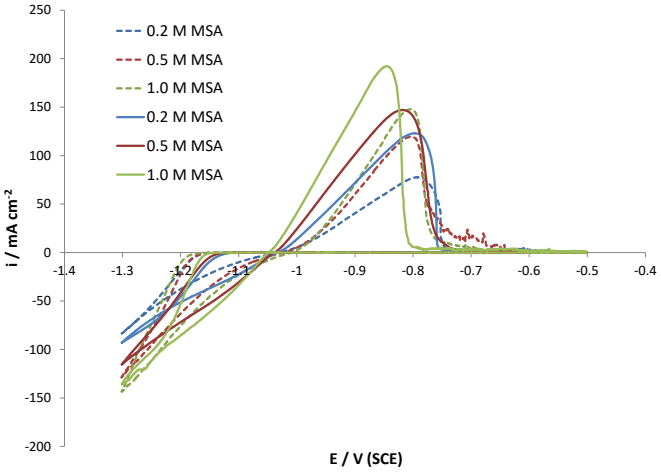

Figure 9: Cyclic voltammograms on a glassy carbon electrode ($\sim$ 0.071 cm^2) obtained in 0.5 $mol\,dm^{-3}$ ZnMSA/0.2 $mol\,dm^{-3}$ $ZnCl_2$ (solid line) and in 0.7 $mol\,dm^{-3}$ electrolyte (dashed line) containing three different MSA base concentrations (0.2, 0.5 and 1.0 $mol\,dm^{-3}$).

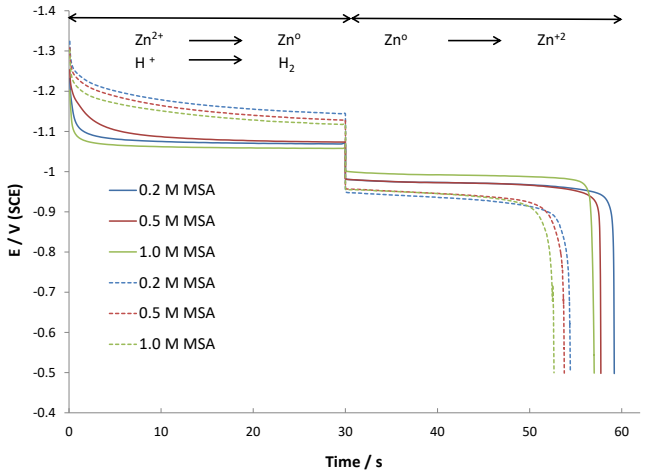

Figure 10: Variation of electrode potential with time during galvanostatic cathodic and anodic polarization of glassy carbon electrode ($\sim$ 0.071 cm^2) at 25 $mA\,cm^{-2}$ in 0.5 $mol\,dm^{-3}$ ZnMSA/0.2 $mol\,dm^{-3}$ $ZnCl_2$ (solid line) and in 0.7 $mol\,dm^{-3}$ electrolyte (dashed line) containing three different MSA base concentrations (0.2, 0.5 and 1.0 $mol\,dm^{-3}$).

3.5.3. *Effect of zinc ion concentration in mixed methanesulfonate/chloride media*

In order to investigate the effect of the Zn(II) concentration on the Zn/Zn(II) system, cyclic voltammograms have been obtained in each of the electrolytes listed in Table 4. In this series of experiments, the total Zn(II) concentration in the mixed electrolyte is increased from 0.7 $\mathrm{mol\,dm^{-3}}$ to 1.0 $\mathrm{mol\,dm^{-3}}$ and 1.5 $\mathrm{mol\,dm^{-3}}$, while the molar ratio of methanesulfonate ions to chloride ions is kept fixed at 5:2. Three solutions with 0.7 $\mathrm{mol\,dm^{-3}}$, 1.0 $\mathrm{mol\,dm^{-3}}$ and 1.5 $\mathrm{mol\,dm^{-3}}$ Zn(II), but in MSA-only electrolytes, are also investigated for comparison purposes. Also, 0.2 $\mathrm{mol\,dm^{-3}}$ MSA has been added to each of these mixed and pure solutions.

Not surprisingly, the cathodic and anodic current density, cumulative charges over the course of the scans of Zn deposition increase as the Zn(II) concentration rises in both electrolytes (Table 5). Also, this change causes the nucleation potential to become more positive. More interesting is the comparison of the effect of the Zn(II) concentration in the two types of electrolytes. E_{nu} is more positive, NOP is smaller, while the amount of metal deposited is larger at each Zn(II) concentration when the process is conducted in the mixed methanesulfonate/chloride electrolyte than in the MSA-only electrolyte. Furthermore, the positive effect of the Zn(II) concentration on the amount of metal deposited is significantly larger in the mixed methanesulfonate/chloride electrolyte than in the MSA-only electrolyte.

Figure 12 shows the effect of the Zn(II) concentration on the electrode potential during the course of galvanostatic cathodic polarization and anodic polarization at 25 $\mathrm{mA\,cm^{-2}}$ in the mixed and pure MSA electrolytes. Obviously, zinc deposition becomes increasingly favored over the HER by the increase in the Zn(II) concentration. Previous studies also found that the charge efficiency increases from 78% in 0.5 $\mathrm{mol\,dm^{-3}}$ Zn(II) to 92% in 2.0 $\mathrm{mol\,dm^{-3}}$ Zn(II) when 1.5 $\mathrm{mol\,dm^{-3}}$ pure MSA electrolyte is used [6]. The transients in Figure 12 show that this leads to less polarization during reduction in both electrolytes

although the effect of the Zn(II) concentration is larger in the MSA-only case. On the other hand, the Zn(II) concentration has no effect on the electrode potential in both solutions as Zn is being oxidized during the anodic polarization. Comparison of the transients also reveals once again the benefits of using the mixed electrolyte over that of the pure MSA electrolyte at each of the Zn(II) levels (less polarization throughout both stages of the cycle, faster attainment of plateau and higher charge efficiency of Zn deposition).

The data in Table 6 reveal that at each Zn(II) concentration, the charge and voltage efficiencies are significantly higher in the mixed electrolyte than in the pure MSA solution. It is desirable to use a higher Zn(II) concentration since this reduces the likelihood that mass transfer will affect battery performance at all states-of-charge and permits the battery to be charged at higher current densities. By using the mixed electrolyte rather than the MSA-only solution, it is possible to achieve a higher energy efficiency with lower nucleation overpotential at high Zn(II) concentrations.

Table 7: Different compositions used to study the effect of Zn(II) concentration in mixed methanesulfonate/chloride and pure MSA electrolytes that also contain 0.2 mol dm^{-3} MSA.

ZnMSA (mol dm^{-3})	$ZnCl_2$ (mol dm^{-3})
0.7	0
1.0	0
1.5	0
0.5	0.2
0.714	0.285
1.072	0.42

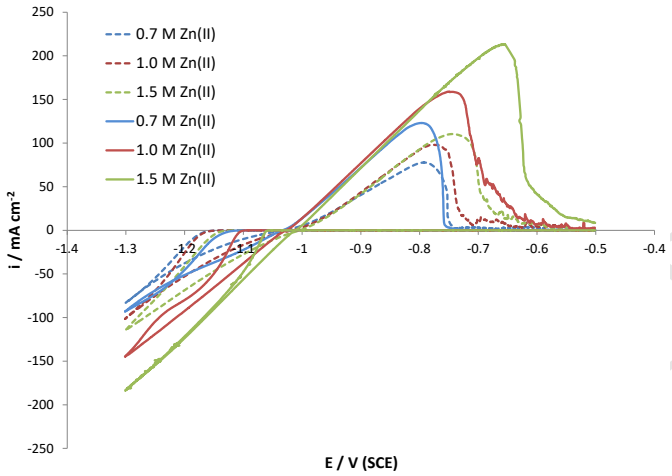

Figure 11: Cyclic voltammograms on a glassy carbon electrode ($\sim$ 0.071 cm^2) obtained in mixed methanesulfonate/chloride media (solid line) and MSA-only electrolyte (dashed line) containing 0.7, 1.0 and 1.5 mol dm^{-3} total Zn(II). The solution compositions are listed in Table 7.

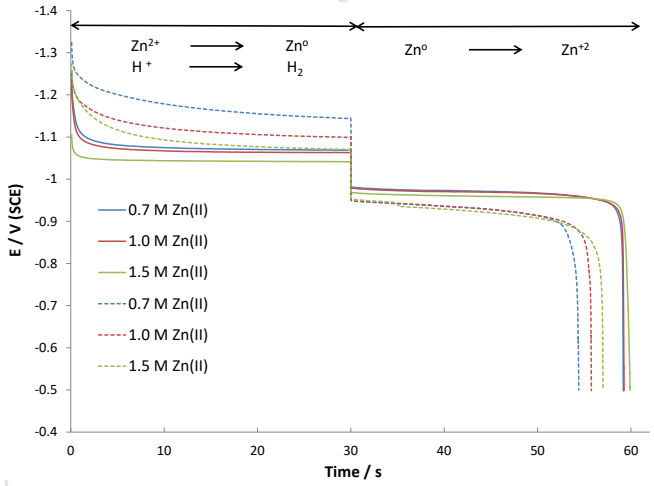

Figure 12: Variation of electrode potential with time during galvanostatic cathodic and anodic polarization of glassy carbon electrode ($\sim$ 0.071 cm^2) at 25 mA cm^{-2} in mixed methanesulfonate/chloride media (solid line) and MSA-only electrolyte (dashed line) containing 0.7, 1.0 and 1.5 mol dm^{-3} total Zn(II). The solution compositions are listed in Table 7.

3.5.4. Effect of current density

Figure 13 shows the effect of current density on the charge/discharge of the zinc redox reaction in solutions containing 1.2 mol dm^{-3} ZnMSA/0.3 mol dm^{-3} $ZnCl_2$ in 1 mol dm^{-3} MSA compared to those obtained in the MSA-only electrolyte (1.5 mol dm^{-3} ZnMSA in 1 mol dm^{-3} MSA). Similar to previous studies [6,18], higher energy efficiency is found at a moderate current density of 25 mA cm^{-2}. The corresponding data in Table 5 show that the voltage efficiency decreases in both types of electrolytes as the current density is increased. Although the VE% is very high at a low current density of 5 mA cm^{-2}, due to the high self-discharge of zinc, the resulting charge efficiency is the lowest. As the current density is raised above 25 mA cm^{-2}, the current efficiency slightly decreases but is generally independent of the applied current density, which is in agreement with previous literature [48]. The data in Table 6 reveal that regardless of the applied current density, the charge, voltage and the resulting energy efficiency are higher in the mixed electrolyte compared to the pure MSA media and the highest energy efficiency is obtained at a current density of 25 mA cm^{-2}.

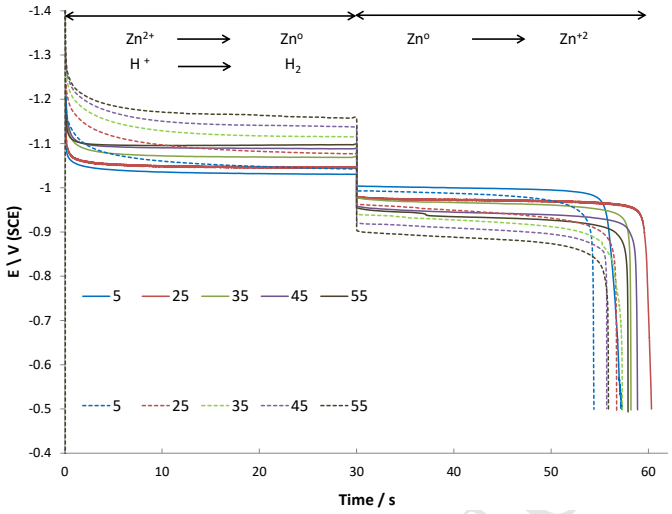

Figure 13: Variation of electrode potential with time during galvanostatic cathodic and anodic polarization of glassy carbon electrode ($\sim$ 0.071 cm^2) in mixed methanesulfonate/chloride media (solid line) and MSA-only electrolyte (dashed line) at different applied current densities. Current densities are in $mA\,cm^{-2}$.

3.6. Deposit morphology

Figure 14 shows the micrographs of zinc deposited from solutions containing 0.5 $mol\,dm^{-3}$ ZnMSA/0.2 $mol\,dm^{-3}$ $ZnCl_2$ compared to those obtained in the MSA-only electrolyte (0.7 $mol\,dm^{-3}$ ZnMSA). The base electrolyte was 0.2 $mol\,dm^{-3}$ MSA for both solutions. During deposition, the parallel hydrogen evolution reaction resulted in hydrogen bubbles covering many sites on the electrode surface. At some sites, these hydrogen bubbles could undercut and dislodge part of the zinc deposit. The poor surface adhesion of zinc onto glassy carbon electrode and the incomplete coverage of the GC electrode surface by zinc deposits have also been reported in a previous study on the comparison of different carbon materials for the negative side of the zinc-cerium redox flow batteries [45]. It should be noted that the use of carbon composite materials such as polyvinyl ester (PVE) and polyvinylidene difluoride (PVDF) largely solves these problems [45].

For both electrolytes, the deposited zinc is made up of hexagonal grains that

are randomly oriented on the electrode surface. This type of morphology for zinc deposits have also been reported in various previous studies [6,18,21]. By comparing the two images, it is clear that the addition of chloride has resulted in denser deposits with a more packed morphology. This is supported by our results in Table 5 which showed that regardless of the operating parameters, the anodic charge (which corresponds to the amount of deposited zinc) is significantly higher in mixed electrolytes than in the pure MSA media.

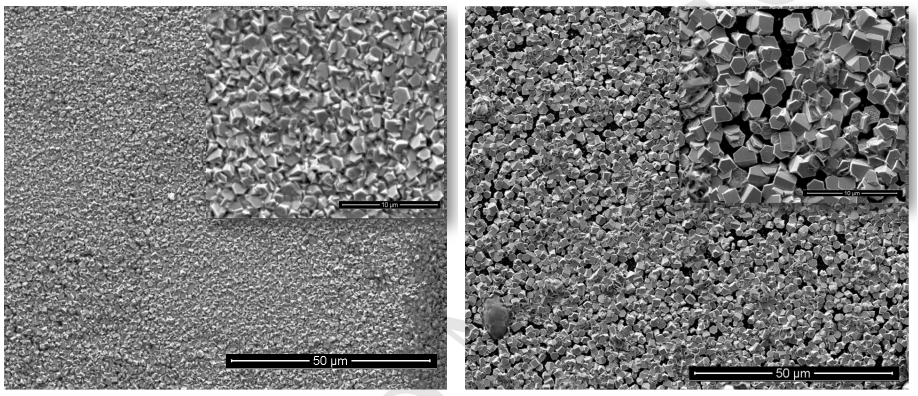

(a) (b)

Figure 14: The SEM images of zinc deposited from (a) 0.5 mol dm^{-3} ZnMSA/0.2 mol dm^{-3} $ZnCl_2$ and (b) 0.7 mol dm^{-3} ZnMSA onto glassy carbon plate ($\sim$ 0.25 cm^2). The deposition was done galvanostatically under constant current of 50 mA cm^{-2} for 1 minute.

4. Conclusions

- Cyclic voltammetry and polarization experiments show that the introduction of moderate concentrations of chloride ions (0.2 – 0.3 mol dm^{-3}) to MSA-based electrolytes leads to a significant increase in the rate and amount of Zn deposition, positive shift in the nucleation potential, reduction in the nucleation overpotential and enhanced exchange current densities.

- The addition of sulfate ions into the MSA-based electrolyte leads to a

lower rate of Zn deposition, slightly higher nucleation overpotential and similar charge efficiency to that attained in MSA-only electrolytes.

- The use of a mixed electrolyte has also been found to improve the transport properties of Zn(II). The diffusion coefficient of Zn(II) is found to be 6.0×10^{-6} $cm^2\,s^{-1}$ in 0.01 $mol\,dm^{-3}$ ZnMSA/0.01 $mol\,dm^{-3}$ $ZnCl_2$ compared to 4.6×10^{-6} $cm^2\,s^{-1}$ in 0.02 $mol\,dm^{-3}$ ZnMSA.

- Both potentiostatic and galvanostatic experiments conducted at 25, 35 and 45°C show that the rate, charge efficiency and voltage efficiency of Zn deposition are higher in the mixed methanesulfonate/chloride solution than in the MSA-only solution at each temperature.

- Although an increase in the base MSA concentration lowers the charge efficiency for Zn deposition in both pure and mixed MSA electrolytes, the use of a mixed methanesulfonate/chloride system leads to higher charge and voltage efficiency than in pure MSA electrolyte.

- The microghraph of zinc deposited from a mixed methansulfonate/chloride solution resulted in more packed morphology compared to the deposits from pure MSA electrolyte.

Since mixed methanesulfonate/chloride electrolytes have also been shown to increase the reversibility and kinetics of the Ce(III)/Ce(IV) half-cell reaction [11], it is also viable to use them as the common electrolytes in undivided zinc-cerium RFBs. However, before any further work on an undivided RFB is done, a thorough study on the effect of Ce(III) and Ce(IV) on the Zn/Zn(II) half-cell reaction is necessary and is the subject of our ongoing research.

Acknowledgement

The authors acknowledge the financial support of the Natural Sciences and Engineering Research Council of Canada (NSERC) through Discovery Grant 170912 which enabled this research to be carried out. They also express their

gratitude to Dr. Neil McManus for providing the glassy carbon electrode used in this research.

References

[1] G. Pleßmann, M. Erdmann, M. Hlusiak, C. Breyer, Global energy storage demand for a 100% renewable electricity supply, Energy Procedia 46 (2014) 22–31. doi:10.1016/j.egypro.2014.01.154.

[2] C. Bussar, M. Moos, R. Alvarez, P. Wolf, T. Thien, H. Chen, Z. Cai, M. Leuthold, D. U. Sauer, A. Moser, Optimal allocation and capacity of energy storage systems in a future european power system with 100% renewable energy generation, Energy Procedia 46 (2014) 40–47. doi:10.1016/j.egypro.2014.01.156.

[3] C. Ponce-de León, A. Frías-Ferrer, J. González-García, D. Szánto, F. C. Walsh, Redox flow cells for energy conversion, Journal of Power Sources 160 (1) (2006) 716–732. doi:10.1016/j.jpowsour.2006.02.095.

[4] R. L. Clarke, B. Dougherty, S. Harrison, P. J. Millington, S. Mohanta, Cerium batteries, US Patent 7,625,663 (Dec. 1 2009).

[5] P. K. Leung, C. Ponce-de León, C. T. J. Low, A. Shah, F. C. Walsh, Characterization of a zinc–cerium flow battery, Journal of Power Sources 196 (11) (2011) 5174–5185.

[6] P. K. Leung, C. Ponce-de León, C. T. J. Low, F. C. Walsh, Zinc deposition and dissolution in methanesulfonic acid onto a carbon composite electrode as the negative electrode reactions in a hybrid redox flow battery, Electrochimica Acta 56 (18) (2011) 6536–6546. doi:10.1016/j.electacta.2011.04.111.

[7] P. K. Leung, C. Ponce-de León, C. T. J. Low, F. C. Walsh, Ce(III)/Ce(IV) in methanesulfonic acid as the positive half cell of a redox flow battery,

Electrochimica Acta 56 (5) (2011) 2145–2153. doi:10.1016/j.electacta.2010.12.038.

[8] M. Matheswaran, S. Balaji, S. J. Chung, I. S. Moon, Electro-oxidation kinetics of cerium (III) in nitric acid using divided electrochemical cell for application in the mediated electrochemical oxidation of phenol, Bulletin-korean chemical society 28 (8) (2007) 1329.

[9] R. P. Kreh, R. M. Spotnitz, J. T. Lundquist, Mediated electrochemical synthesis of aromatic aldehydes, ketones, and quinones using ceric methanesulfonate, The Journal of Organic Chemistry 54 (7) (1989) 1526–1531.

[10] Z. Xie, F. Xiong, D. Zhou, Study of the Ce^{3+}/Ce^{4+} redox couple in mixed-acid media (CH_3SO_3H and H_2SO_4) for redox flow battery application, Energy & Fuels 25 (5) (2011) 2399–2404. doi:10.1021/ef200354b.

[11] G. Nikiforidis, W. A. Daoud, Effect of mixed acid media on the positive side of the hybrid zinc-cerium redox flow battery, Electrochimica Acta 141 (2014) 255–262. doi:10.1016/j.electacta.2014.06.142.

[12] S. Peng, N.-F. Wang, X.-J. Wu, S.-Q. Liu, D. Fang, Y.-N. Liu, K.-L. Huang, Vanadium species in CH_3SO_3H and H_2SO_4 mixed acid as the supporting electrolyte for vanadium redox flow battery, International Journal of Electrochemical Science 7 (1) (2012) 643–649.

[13] S. Kim, E. Thomsen, G. Xia, Z. Nie, J. Bao, K. Recknagle, W. Wang, V. Viswanathan, Q. Luo, X. Wei, A. Crawford, G. Coffey, G. Maupin, V. Sprenkle, 1 kW/1 kWh advanced vanadium redox flow battery utilizing mixed acid electrolytes, Journal of Power Sources 237 (2013) 300–309. doi:10.1016/j.jpowsour.2013.02.045.

[14] S. Kim, M. Vijayakumar, W. Wang, J. Zhang, B. Chen, Z. Nie, F. Chen, J. Hu, L. Li, Z. Yang, Chloride supporting electrolytes for all-vanadium redox flow batteries, Physical Chemistry Chemical Physics 13 (40) (2011) 18186. doi:10.1039/c1cp22638j.

[15] P. K. Leung, C. Ponce-de León, F. C. Walsh, An undivided zinc–cerium redox flow battery operating at room temperature (295 k), Electrochemistry Communications 13 (8) (2011) 770–773. doi:10.1016/j.elecom.2011.04.011.

[16] P. K. Leung, C. Ponce-de León, F. C. Walsh, The influence of operational parameters on the performance of an undivided zinc–cerium flow battery, Electrochimica Acta 80 (2012) 7–14.

[17] L. F. Arenas, F. C. Walsh, C. Ponce-de León, The importance of cell geometry and electrolyte properties to the cell potential of zn-ce hybrid flow batteries, Journal of The Electrochemical Society 163 (1) (2016) A5170–A5179.

[18] J. Pan, Y. Wen, J. Cheng, J. Pan, Z. Bai, Y. Yang, Zinc deposition and dissolution in sulfuric acid onto a graphite–resin composite electrode as the negative electrode reactions in acidic zinc-based redox flow batteries, Journal of Applied Electrochemistry 43 (5) (2013) 541–551. doi:10.1007/s10800-013-0538-1.

[19] C. Cachet, R. Wiart, Zinc deposition and passivated hydrogen evolution in highly acidic sulphate electrolytes: Depassivation by nickel impurities (nov 1990). doi:10.1007/bf01019581.

[20] I. Zouari, F. Lapicque, An electrochemical study of zinc deposition in a sulfate medium, Electrochimica Acta 37 (3) (1992) 439–446. doi:10.1016/0013-4686(92)87033-v.

[21] J. Yu, H. Yang, X. Ai, Y. Chen, Effects of anions on the zinc electrodeposition onto glassy-carbon electrode, Russian journal of electrochemistry 38 (3) (2002) 321–325.

[22] G. Trejo, Nucleation and growth of zinc from chloride concentrated solutions, Journal of The Electrochemical Society 145 (12) (1998) 4090. doi:10.1149/1.1838919.

[23] J. Mcbreen, E. Gannon, ChemInform abstract: Electrodeposition of zinc on glassy carbon from zinc chloride and zinc bromide electrolytes, Chemischer Informationsdienst 14 (49) (1983) 47. doi:10.1002/chin.198349021.

[24] L. H. Mendoza-Huízar, C. H. Rios-Reyes, M. G. Gómez-Villegas, Zinc electrodeposition from chloride solutions onto glassy carbon electrode, Journal of the Mexican Chemical Society 53 (4) (2009) 243–247.

[25] G. Nikiforidis, L. Berlouis, D. Hall, D. Hodgson, Evaluation of carbon composite materials for the negative electrode in the zinc–cerium redox flow cell, Journal of Power Sources 206 (2012) 497–503.

[26] H. Nakamura, S. Oue, N. Sogabe, H. Nakano, Effect of chloride ions on the deposition behavior and morphology of zinc at initial stage from electrowinning solution, Journal of MMIJ 131 (5) (2015) 164–169. doi:10.2473/journalofmmij.131.164.

[27] J. Yeager, J. P. Cels, E. Yeager, F. Hovorka, The electrochemistry of nickel i. codeposition of nickel and hydrogen from simple aqueous solutions, Journal of the electrochemical society 106 (4) (1959) 328–336.

[28] Z. Nagy, Chloride ion catalysis of the copper deposition reaction, Journal of The Electrochemical Society 142 (6) (1995) L87. doi:10.1149/1.2044254.

[29] R. L. Pecsok, J. J. Lingane, Polarography of chromium (II), Journal of the American Chemical Society 72 (1) (1950) 189–193.

[30] J. Heyrovský, Retarded electrodeposition of metals studied oscillographically with mercury capillary electrodes, Discussions of the Faraday Society 1 (1947) 212. doi:10.1039/df9470100212.

[31] J. Vazquez-Arenas, M. Pritzker, Effect of electrolyte and agitation on the anomalous behavior and morphology of electrodeposited Co–Ni alloys, Journal of Solid State Electrochemistry 17 (2) (2012) 419–433. doi:10.1007/s10008-012-1932-z.

[32] V. Gouda, M. Khedr, A. S. El Din, Role of anions in the corrosion and corrosion-inhibition of zinc in aqueous solutions, Corrosion Science 7 (4) (1967) 221–230.

[33] J. Blackledge, N.-S. Hush, Mechanism of the Zn(II)/Zn(Hg) exchange: Part 2: catalysis by halide and thiocyanatk ions, Journal of Electroanalytical Chemistry (1959) 5 (6) (1963) 435–449.

[34] E. Ahlberg, H. Anderson, Simulating impedance spectra from a mechanistic point of view: application to zinc dissolution, Acta Chemica Scandinavica(Denmark) 46 (1) (1992) 15–24.

[35] G. Nikiforidis, W. A. Daoud, Indium modified graphite electrodes on highly zinc containing methanesulfonate electrolyte for zinc-cerium redox flow battery, Electrochimica Acta 168 (2015) 394–402.

[36] S. Ranganathan, T.-C. Kuo, R. L. McCreery, Facile preparation of active glassy carbon electrodes with activated carbon and organic solvents, Analytical Chemistry 71 (16) (1999) 3574–3580. doi:10.1021/ac981386n.

[37] M. D. Gernon, M. Wu, T. Buszta, P. Janney, Environmental benefits of methanesulfonic acid, Green Chemistry 1 (3) (1999) 127–140. doi:10.1039/a900157c.

[38] Q. B. Zhang, Y. Hua, Effect of Mn^{2+} ions on the electrodeposition of zinc from acidic sulphate solutions, Hydrometallurgy 99 (3-4) (2009) 249–254. doi:10.1016/j.hydromet.2009.09.002.

[39] R. de Levie, Anion bridging and anion electrocatalysis on mercury, Journal of The Electrochemical Society 118 (8) (1971) 185C. doi:10.1149/1.2408333.

[40] L. G. Sillén, A. E. Martell, Stability constants of metallic-ion complexes, Soil Science 100 (1) (1965) 74. doi:10.1097/00010694-196507000-00026.

[41] M. Capelato, J. Nobrega, E. Neves, Complexing power of alkanesulfonate ions: the lead-methanesulfonate syste, Journal of Applied Electrochemistry 25 (4) (1995) 74. doi:10.1007/bf00249661.

[42] F. I. Danilov, I. V. Sknar, Y. E. Sknar, Kinetics of nickel electroplating from methanesulfonate electrolyte, Russian Journal of Electrochemistry 47 (9) (2011) 1035–1042. doi:10.1134/s1023193511090114.

[43] P. K. Leung, C. Ponce-de León, F. Recio, P. Herrasti, F. C. Walsh, Corrosion of the zinc negative electrode of zinc–cerium hybrid redox flow batteries in methanesulfonic acid, Journal of Applied Electrochemistry 44 (9) (2014) 1025–1035.

[44] D. Baik, D. Fray, Electrodeposition of zinc from high acid zinc chloride solutions, Journal of applied electrochemistry 31 (10) (2001) 1141–1147.

[45] G. Nikiforidis, L. Berlouis, D. Hall, D. Hodgson, A study of different carbon composite materials for the negative half-cell reaction of the zinc cerium hybrid redox flow cell, Electrochimica Acta 113 (2013) 412–423.

[46] V. G. Levich, Physicochemical hydrodynamics, Prentice hall, 1962.

[47] E. B. Budevski, Deposition and dissolution of metals and alloys. part a: Electrocrystallization, in: Comprehensive treatise of electrochemistry, Springer, 1983, pp. 399–450.

[48] Q. B. Zhang, Y. X. Hua, T. G. Dong, D. G. Zhou, Effects of temperature and current density on zinc electrodeposition from acidic sulfate electrolyte with [BMIM] HSO_4 as additive, Journal of applied electrochemistry 39 (8) (2009) 1207.

Electrodeposition and Electrodissolution of Zinc in Mixed Methanesulfonate-Based Electrolytes

Kiana Amini, Mark D. Pritzker*

Department of Chemical Engineering, University of Waterloo, 200 University Avenue West, Waterloo, Ontario, Canada N2L 3G1

Abstract

Zinc electrodeposition and electrodissolution in methanesulfonic acid (MSA) electrolytes mixed with chloride or sulfate are investigated in a 3-electrode cell for eventual use in divided and undivided zinc-cerium redox flow batteries (RFB). Cyclic voltammetry and linear polarization experiments show that the addition of chloride to methanesulfonate-based electrolytes shifts the nucleation potential in the positive direction, lowers the nucleation overpotential and enhances the kinetics of Zn deposition and subsequent dissolution relative to that achieved when sulfate is added or MSA is the only anion present. In addition, the diffusion coefficient of Zn(II) and the resulting limiting current density for Zn deposition have been found to be moderately higher in mixed methanesulfonate/chloride media than when chloride is absent. The effects of temperature, MSA concentration, Zn(II) concentration and current density on the Zn/Zn(II) system have also been investigated under potentiostatic and galvanostatic conditions. Although an increase in temperature and/or MSA concentration tends to lower the charge efficiency for Zn deposition in both mixed and MSA-only electrolytes due to the higher rate of hydrogen evolution, the amount of zinc deposited, charge and voltage efficiency always remain significantly higher in the mixed methanesulfonate/chloride media than the pure MSA media. Thus, the use of a mixed methanesulfonate/chloride media should enable both divided

*Corresponding author. Tel.: +1 519 888 4567 x32542
Email address: pritzker@uwaterloo.ca (Mark D. Pritzker)

and undivided zinc-cerium RFBs to operate over a wider range of temperatures and MSA concentrations compared to the case with pure MSA electrolyte. The addition of sulfate to MSA-based electrolytes, however, does not improve the performance of the Zn/Zn(II) system relative to that possible in the MSA-only electrolytes.

Keywords: deposition, dissolution, mixed electrolyte, redox flow battery, zinc

1. Introduction

In the last few years, the interest in energy storage devices has intensified [1,2]. A reliable and cost-effective energy storage unit can dramatically enhance the integration of renewable energies such as solar and wind into the electrical grid and can smooth out the large inherent fluctuations in the availability of these sources. The energy produced from renewable sources under the proper conditions (time and climate) can be stored in a storage unit and discharged during periods of high demand. If successful, these storage devices will enable the electrical grid to be far less reliant on energy sources such as fossil fuels that are responsible for major environmental problems (climate change, acid rain, air pollution).

One of the most recent and promising technologies for energy storage are redox flow batteries (RFB). Since the active material in RFBs is stored externally from the cell in storage tanks, the energy and power of such batteries are independent and so they can be scaled up more easily than other types of storage devices [3]. Over the past decades, different RFB systems have been developed. Among these systems, zinc-based RFBs have gained a great deal of attention due to the availability and low price of zinc and the successful use of zinc electrodes in many other battery systems. More importantly, the zinc redox couple provides a large negative potential in aqueous media with a two-electron transfer reaction. Zinc-cerium RFBs are relatively new systems developed by Plurion Inc. [4]. This system offers the highest open-circuit voltage (2.4 V) among the other RFBs, which can lead to high energy densities when the elec-

trolyte contains high concentrations of the electroactive species. In this battery, methanesulfonic acid (MSA) has been used as the supporting electrolyte for both the negative Zn/Zn(II) and positive Ce(III)/Ce(IV) half-cells. Divided two-compartment zinc-cerium RFB cells have been operated with 0.8 mol dm^{-3} cerous methanesulfonate dissolved in 4 mol dm^{-3} MSA for the positive half-cell and 1.5 mol dm^{-3} zinc methanesulfonate in 1 mol dm^{-3} MSA for the negative half-cell [5]. Lower MSA concentrations are used in the negative half-cell since higher concentrations lead to lower zinc deposition/dissolution efficiencies due to competition from the hydrogen evolution reaction [6]. This battery has been operated at 40-60°C [7] due to the higher reversibility and improved kinetics of the Ce(III)/Ce(IV) redox couple at higher temperatures [7], [8].

Despite these advantages, the zinc-cerium system faces a number of obstacles that must be overcome if RFBs based on this chemistry are to become commercially feasible. This has led to considerable research activity on this system in recent years. Despite its favourable thermodynamics, the Ce(III)/Ce(IV) redox reaction has sluggish kinetics [7]. The solubility of Ce(III) rises as the MSA concentration is reduced, whereas the solubility of Ce(IV) is affected in the opposite way [9]. Thus, a compromise must be made to maintain high solubility of both cerium species in the electrolyte. In order to improve the reversibility and kinetics of the Ce(III)/Ce(IV) redox couple and solubility of both cerium species, the use of a mixed-electrolyte media has been investigated as a potential remedy [10,11]. The addition of moderate concentrations (0.5 – 1 mol dm^{-3}) of hydrochloric acid to the base MSA electrolyte has been shown to significantly improve the reversibility and kinetics of the Ce(III)/Ce(IV) redox reaction [11]. Moreover, the diffusion coefficient of Ce(III) was also found to be enhanced in these mixed electrolytes [11]. Although the presence of sulfate rather than chloride in mixed methanesulfonate media also has a positive influence on the Ce(III)/Ce(IV) reaction, its effect does not appear to be as strong [11]. One beneficial effect is an increase in the solubility of Ce(IV) to 1.0 mol dm^{-3} in 2 mol dm^{-3} methanesulfonate / 0.5 mol dm^{-3} sulfate solution [10], while it is less than 0.5 mol dm^{-3} in 2.5 mol dm^{-3} pure MSA electrolyte [9]. The introduction

of a mixed acid media has also been used in all-vanadium redox flow batteries and also found to have positive effects [12,13]. A mixed chloride/sulfate electrolyte enhanced the operating temperature range and stability of vanadium species which was attributed to the formation of stable and soluble vanadium-chloride intermediate complexes [14].

Leung et al. have investigated the use of a membrane-less single compartment zinc-cerium RFB [15]. Elimination of the expensive ion-exchange membrane from RFBs is a very attractive option since it would significantly reduce the cost of materials, simplify the design of the battery and reduce the ohmic resistance across the cell. Moreover, the proposed undivided zinc/cerium RFB is operated at room temperature [15], which is more desirable than the 50°C considered for a divided zinc/cerium RFB [5]. As mentioned before, a high MSA concentration is required for a high solubility of Ce(IV) [9], while the efficiency of zinc deposition/dissolution reaction decreases at high MSA concentrations due to excessive hydrogen evolution [6]. Thus, in a membrane-less battery where a single electrolyte is used, a compromise must be made between a high Ce(IV) solubility and high efficiency of the Zn/Zn(II) redox reaction. Consequently, membrane-less zinc-cerium RFBs have been operated at lower acid concentrations ($\sim$ 0.2 $\mathrm{mol\,dm^{-3}}$ – 0.5 $\mathrm{mol\,dm^{-3}}$) and lower Ce concentrations (0.2 $\mathrm{mol\,dm^{-3}}$ – 0.4 $\mathrm{mol\,dm^{-3}}$ Ce(III)) [15,16]. The most successful undivided battery to date has reportedly achieved a current efficiency of 90% and an energy efficiency of 75% at 20 $\mathrm{mA\,cm^{-2}}$ [15].

As mentioned previously, mixed-acid media, particularly MSA-chloride electrolyte, have been shown to significantly enhance the reversibility and kinetics of the Ce(III)/Ce(IV) half-cell reaction [11]. Hence, we expect that it would be beneficial to use such mixed-acid media in a membrane-less zinc-cerium RFB as well. Since both electrodes and half-cells are exposed to the same electrolyte in a membrane-less RFB, it is essential to first investigate the influence of such mixed electrolytes on the zinc deposition and dissolution reactions that occur at the negative electrode during the charge and discharge of a zinc-cerium RFB.

The Zn/Zn(II) half-cell reaction has been studied in methanesulfonic [6,17],

sulfuric [18,19,20,21] and chloride [21,22,23] baths. However, to the best of our knowledge, no study on this system in a mixed electrolyte has been reported. The standard rate constant reported in pure chloride solutions is 8.78×10^{-3} $\mathrm{cm\,s^{-1}}$ [24], which is about an order of magnitude higher than the value of 0.16×10^{-3} $\mathrm{cm\,s^{-1}}$ obtained in MSA-only electrolytes [25]. This reflects the beneficial role of chlorides in enhancing the kinetics of the zinc redox reaction. Based on the well-known behavior of metal deposition systems in general, we expect that the addition of chloride ions to the base MSA electrolyte will be beneficial to zinc deposition. It has been reported that the presence of chloride in zinc electrowinning baths leads to lower polarization resistance and higher charge efficiency of zinc deposition [26]. Additionally, cyclic voltammetry experiments have shown that the overpotential is reduced and the cathodic peak potential is shifted in the positive direction when zinc deposition is carried out in chloride-only baths rather than sulfate-only electrolytes [21]. Chloride ions have also improved the deposition performance of other metals and alloys such as nickel [27], copper [28], chromium [29], indium [30] and Co-Ni alloys [31]. Thus, it is reasonable to investigate the use of chloride ions to facilitate the zinc deposition process.

In terms of the effect of electrolyte composition on zinc electrodissolution, a thermometric study has shown that both chloride and sulfate tend to promote the oxidation of zinc in acidic media and should be considered as corrosive anions although it was not possible to easily differentiate between their relative strengths as corrosion promoters [32]. Although the effect of chloride on zinc dissolution in highly acidic methanesulfonate-based electrolytes has not been reported to date, halogens including chloride have been shown to increase the rate of the Zn(II)/Zn(Hg) reduction and oxidation reaction when they are added to a $NaClO_4$ base electrolyte [33], [34].

In this experimental study, we use a 3-electrode system to determine the electrolyte composition and operating conditions that optimize the kinetics of zinc electrodeposition and electrodissolution in mixed-electrolyte media with particular emphasis on methanesulfonate/chloride solutions. Carbon electrodes

have been commonly used in RFB systems due to their chemically inert nature. In some applications, the carbon electrode must be coated to avoid corrosion by corrosive ions (i.e. cerium in the case of an undivided zinc cerium RFB). Moreover, the negative electrode can be modified to inhibit undesired side reactions. For example, indium-modified graphite electrodes can be used on the negative side of the zinc-cerium RFBs to reduce hydrogen evolution [35]. In this work, we use a glassy carbon disk electrode as the working electrode. Since the ultimate aim is to determine the optimum operating conditions for a zinc-cerium RFB, we apply compositions that are typically used for this application. The undivided zinc-cerium RFBs are operated at lower acid concentrations ($\sim$ 0.2 $\mathrm{mol\,dm^{-3}}$ – 0.5 $\mathrm{mol\,dm^{-3}}$ MSA base electrolyte) [15,16], while the negative half-cell of a divided zinc-cerium RFB typically contains a higher acid concentration of $\sim$ 1 $\mathrm{mol\,dm^{-3}}$ MSA. Thus, in order to address both possible situations, we investigate Zn electrodeposition/electrodissolution in two sets of solutions containing either 0.2 $\mathrm{mol\,dm^{-3}}$ or 1 $\mathrm{mol\,dm^{-3}}$ MSA base electrolyte. In particular, the effects of temperature, acid concentration and Zn(II) concentration on the behavior of the Zn/Zn(II) system in mixed-electrolyte media are determined.

2. Experimental

For these experiments, a custom-made three-electrode water-jacketed glass cell (Adams & Chittenden Scientific Glass) was employed. The capacity of the cell is $\sim$ 200 ml and the outer cell has the dimensions of 110 mm diameter $\times$ 55 mm height. This cell was connected to a circulating bath (Neslab RTE-8) to control the electrolyte temperature throughout the experiments. All electrochemical experiments were carried out using an EPP-400 potentiostat (Princeton Applied Research). The reference electrode was a saturated glass body calomel electrode (Fisher Scientific) and the counter electrode was a graphite rod (6.15 mm diameter $\times$ 50 mm long). All electrode potentials reported herein correspond to the SCE scale. The working electrode was a glassy carbon (GC) disk of 3 mm diameter (area $\sim$ 0.071 $\mathrm{cm^2}$). The GC electrode tip has a PTFE

holder that was fitted to the EDI101 rotator and CTV speed control unit (Radiometer Analytical) for the rotating disk electrode (RDE) experiments. The GC electrode was polished manually with 0.05 µm alumina powder (Buehler) on a MicroCloth polishing pad (Buehler) for several minutes to a mirror finish prior to each experiment. The electrode was then rinsed thoroughly with ultra-pure water (resistivity $\sim$ 18 MΩ cm). It has been shown that the ferricyanide/ferrocyanide redox reaction is sensitive to the cleanliness and preparation method of GC electrodes [36]. Thus, the cleanliness of the GC electrode was assessed by carrying out a cyclic voltammetry scan first from 0.6 to 0 V *vs* SCE and then reversing back to 0.6 V at a scan rate of 100 mV s^{-1} in a solution containing 1 mmol dm^{-3} ferricyanide and 1 mol dm^{-3} KCl and measuring the separation between the cathodic and anodic potential peaks for the ferricyanide/ferrocyanide redox couple. Ideally the separation should be close to 60 mV, as expected for a 1-electron reaction. We measured the peak separation using our clean GC electrode to be 69 mV, which is close to the reported value. After each test with ferricyanide, the electrode surface was again rinsed thoroughly with water.

All solutions used for the zinc deposition/dissolution experiments were prepared with analytical grade reagents and ultra-pure water (resistivity $\sim$ 18 MΩ cm). To prevent possible interference from the oxygen reduction reaction, the solutions were purged with nitrogen gas prior to each deposition experiment for 10 minutes and the subsequent experiments were conducted under a blanket of nitrogen gas. The zinc(II) methanesulfonate solutions were prepared by dissolving the appropriate amounts of high purity zinc oxide (Zochem Inc.) in 70% methanesulfonic acid (Alfa Aesar), while sodium methanesulfonate solutions were prepared by dissolving sodium carbonate decahydrate (Alfa Aesar) in 70% methanesulfonic acid. The resulting solutions were colorless with no sign of any precipitate forming. Anhydrous zinc chloride (99% purity; Fisher Scientific) and zinc sulfate heptahydrate (98% purity; Alfa Aesar) were added to these solutions in order to introduce the chloride and sulfate ions into the mixed-electrolyte media. In order to compare the mixed-electrolyte media with

pure chloride and sulfate baths, solutions were also made with hydrochloric acid (Sigma Aldrich) and sulfuric acid (Sigma Aldrich) instead of methanesulfonic acid. Solutions that contain MSA, HCl and H_2SO_4 have a pH close to zero. In order to increase the pH of the solutions to higher values (pH 4) for the RDE experiments, 0.5 mol dm^{-3} sodium methanesulfonate, sodium chloride (EMD Millipore) and sodium sulfate (EMD Millipore) were added to the sulfonic-, chloride- and sulfate-based solutions, respectively, followed by the appropriate amounts of MSA, HCl and H_2SO_4, respectively. The kinematic viscosity of the solutions was measured using a Cannon-Fenske viscometer tube. The pH of the solutions was measured with an Orion (420A) pH meter.

The electrochemical techniques conducted included cyclic voltammetry, linear polarization and galvanostatic deposition/dissolution under unstirred conditions and linear sweep voltammetry using a rotating disk electrode. Zinc deposition onto the GC electrode was carried out galvanostatically for 30 seconds at a constant current density of 25 mA cm^{-2}, followed by zinc dissolution with the same current density. To prevent excessive oxidation of the electrode surface, zinc dissolution was halted when the potential shifted to values more positive than -0.5 versus SCE. For the morphology study, deposition onto a glassy carbon plate (Alfa Aesar) was carried out. The plate was taped with an insulating polyester tape (Cole-Parmer) to ensure that the area of the working electrode exposed to the solution was 0.5 $\times$ 0.5 cm^2. In this case, zinc deposition was done galvanostatically at a current density of 50 mA cm^{-2} for 1 minute. The images of the deposits were taken with a scanning electron microscope model Zeiss FESEM 1530.

3. Results and Discussion

Table 1 shows the compositions of the different electrolytes investigated in this study. As can be seen, MSA is the base acid in most of the samples. MSA is less corrosive than hydrochloric acid and sulfuric acid, but has comparable conductivity [37]. Moreover, only moderately high concentrations of chloride

are suitable for the electrolyte to be used in a membrane-less zinc-cerium RFB due to the possibility of chlorine gas forming in the presence of Ce(IV). Also, it has been reported that the solubility of Ce(III) in sulfate baths is considerably lower than in MSA media [9]. With these considerations, MSA is the better choice as the base electrolyte.

Table 1: Electrolyte compositions investigated in this study

Low acid concentration			
Base electrolyte ($mol\,dm^{-3}$)	ZnMSA ($mol\,dm^{-3}$)	$ZnCl_2$ ($mol\,dm^{-3}$)	$ZnSO_4$ ($mol\,dm^{-3}$)
0.2 MSA	0.7	0	0
0.2 MSA	0.5	0.2	0
0.2 MSA	0.5	0	0.2
0.2 MSA	0.3	0.4	0
0.2 MSA	0.3	0	0.4
0.2 HCl*	0	0.7	0
0.2 H_2SO_4*	0	0	0.7
High acid concentration			
1.0 MSA	1.5	0	-
1.0 MSA	1.3	0.2	-
1.0 MSA	1.2	0.3	-
1.0 HCl*	0	1.5	-

* For comparison

Since undivided zinc-cerium RFBs are usually operated at lower acid concentrations [15,16], a 0.2 $mol\,dm^{-3}$ MSA base electrolyte containing a total of 0.7 $mol\,dm^{-3}$ Zn(II) is used for one series of voltammetry experiments (Table 1). The total Zn(II) concentration is kept fixed in order to fairly compare the results obtained in the various solutions. For this series of experiments, solutions with mixed methanesulfonate/sulfate have also been prepared since it has been reported that the solubility of Ce(IV) increases in the mixed methanesulfonate/sulfate system [10] which would be beneficial for an undivided zinc-cerium RFB. On the other hand, divided zinc-cerium RFBs operate at much higher

Zn(II) concentrations (1.5 mol dm^{-3} ZnMSA in 1 mol dm^{-3} MSA [5]). Thus, 1 mol dm^{-3} MSA base electrolytes containing a total of 1.5 mol dm^{-3} Zn(II) are used for another series of voltammetry experiments (Table 1).

3.1. Effect of mixed methanesulfonate/chloride electrolyte

Figure 1 shows the cyclic voltammograms obtained in the different mixed methanesulfonate/chloride electrolytes with a total of 0.7 mol dm^{-3} Zn(II) in 0.2 mol dm^{-3} MSA (Table 1) at 25°C on a static glassy carbon electrode. The potential is swept first from -0.5 to -1.3 V *vs* SCE and then reversed back to -0.5 V at a scan rate of 20 mV s^{-1}. A nucleation loop appears during the cathodic scan obtained in each solution and is typical of that observed during metal electrodeposition. In each case, an oxidation peak during the reverse scan arises due to the anodic stripping of Zn(II) into the solution from the metal coating deposited during the previous cathodic portion of the scan.

The voltammograms clearly show that the addition of chloride ions to the electrolyte significantly increases the cathodic and anodic current densities at any particular potential during the scans and decreases the nucleation overpotential (NOP). The NOP is the difference between the nucleation potential E_{nu} (point A) at which cathodic current is first observed during the scan and the crossover potential E_{co} (point B) at which the current switches from cathodic to anodic during the reverse scan and represents the degree of polarization of the cathode [38]. As shown in Table 2, the reduction in the NOP obtained in the mixed methanesulfonate/chloride electrolytes containing a total of 0.7 mol dm^{-3} Zn(II) relative to that in the MSA-only solution reaches as high as 50 mV. The amount of zinc deposited during the cathodic portion of each scan can be determined by measurement of the anodic charge (Q_{an}) during the reverse scan. Analysis of the CVs in Figure 1 shows that the amount of zinc deposited has increased by 57% and 129% when 0.2 and 0.4 mol dm^{-3} chloride ion, respectively, replace MSA in the electrolyte (Table 2). Note that the total Zn(II) concentration is kept fixed at 0.7 mol dm^{-3} in these solutions so that these differences can be attributed to the amount of chloride present.

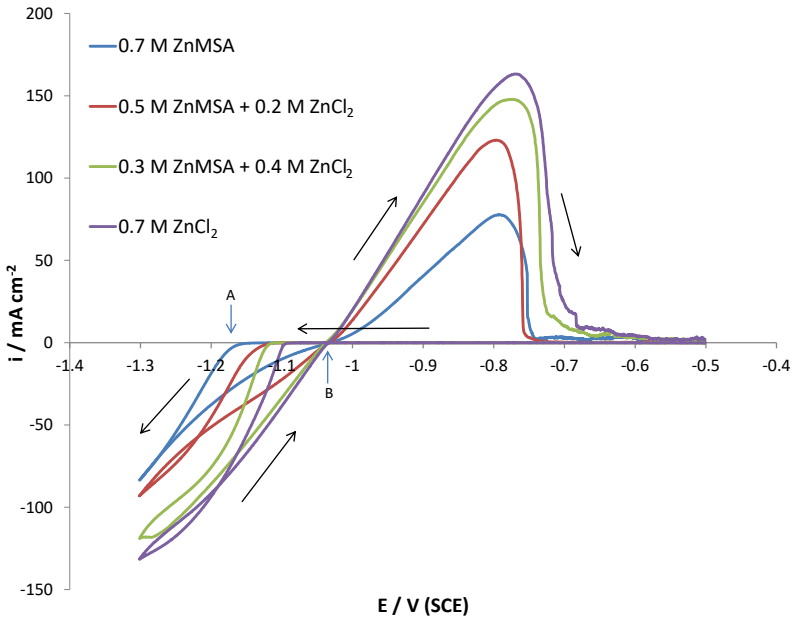

Figure 1: Cyclic voltammograms on a glassy carbon electrode (~ 0.071 cm^2) in different mixed methanesulfonate/chloride media with 0.2 mol dm^{-3} MSA base electrolyte at 25°C and a scan rate of 20 mV s^{-1}.

A similar trend is observed in the cyclic voltammograms in Figure 2 obtained in the different mixed methanesulfonate/chloride electrolytes listed in Table 1 which contain a total of 1.5 mol dm^{-3} Zn(II) in 1 mol dm^{-3} MSA (typical composition of the negative half-cell in divided RFBs). As shown in Table 2, the NOP decreases by 90 mV when 0.3 mol dm^{-3} chloride ion substitutes for MSA in the electrolyte. Furthermore, Q_{an} increases by 113% relative to the value obtained in the 1.5 mol dm^{-3} ZnMSA solution when MSA is replaced by 0.2 mol dm^{-3} chloride and by 179% when it is replaced by 0.3 mol dm^{-3} chloride.

Due to the highly acidic environment of the studied electrolytes, hydrogen evolution (HER) also accompanies zinc deposition during cathodic polarization. In order to determine if the higher cathodic current density obtained in the mixed methanesulfonate/chloride media is due to zinc deposition or hydrogen

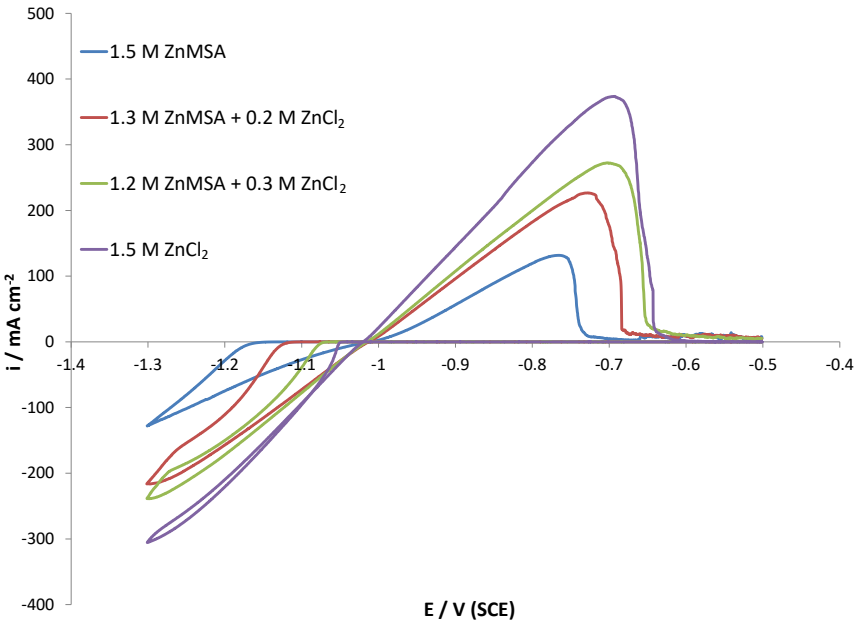

Figure 2: Cyclic voltammograms on a glassy carbon electrode (~ 0.071 cm^2) in different mixed methanesulfonate/chloride media with 1.0 mol dm^{-3} MSA base electrolyte at 25°C and a scan rate of 20 mV s^{-1}.

evolution, the charge efficiency (CE) over each of the voltammograms has been determined and included in Table 2. The charge efficiency is calculated as the ratio of the charge passed during the anodic portion of the scan to that obtained during the cathodic portion. Table 2 shows that higher charge efficiency is achieved in the mixed-electrolyte media than in the MSA-only electrolyte. Thus, the mixed methanesulfonate/chloride electrolyte does not appear to promote the HER and the higher current densities observed in the presence of chloride can be attributed to an increase in the zinc deposition/dissolution rate.

Although a higher concentration of chloride ions in the mixed-electrolyte media improves the zinc half-cell reaction kinetics, it would be preferable to maintain the Cl^- concentration at lower levels in a membrane-less zinc-cerium RFB due to the concern that it could be oxidized by Ce(IV) also present in the electrolyte. Thus, based on the results of this section, a composition of

Table 2: Effect of electrolyte composition on E_{nu}, NOP, Q_{an} and CE of zinc deposition in mixed electrolyte solutions compared to pure methanesulfonate, chloride and sulfate solutions.

Composition (mol dm^{-3})	E_{nu} (V)	-NOP (mV)	Q_{an} (mA s)	CE (%)
0.2 mol dm^{-3} MSA base electrolyte				
0.7 ZnMSA	-1.15	120	42.9	85
0.5 ZnMSA+ 0.2 $ZnCl_2$	-1.11	80	67.4	93
0.3 ZnMSA + 0.4 $ZnCl_2$	-1.11	70	98.4	89
0.7 $ZnCl_2$	-1.09	60	114.2	88
0.5 ZnMSA+ 0.2 $ZnSO_4$	-1.17	130	27.1	88
0.3 ZnMSA+ 0.4 $ZnSO_4$	-1.17	130	25.2	85
0.7 $ZnSO_4$	-1.18	130	31.3	89
1.0 mol dm^{-3} MSA base electrolyte				
1.5 ZnMSA	-1.15	140	73.4	83
1.3 ZnMSA+ 0.2 $ZnCl_2$	-1.11	100	156.1	94
1.2 ZnMSA + 0.3 $ZnCl_2$	-1.07	50	204.8	90
1.5 $ZnCl_2$	-1.05	30	277.7	87

0.5 mol dm^{-3} ZnMSA/0.2 mol dm^{-3} $ZnCl_2$ in 0.2 mol dm^{-3} MSA is chosen for subsequent analysis as an electrolyte in an undivided RFB (see section 3.4). For a divided zinc-cerium RFB, higher chloride concentrations can be used with the MSA base electrolyte. Thus, for this application, we will focus on the composition of 1.2 mol dm^{-3} ZnMSA/0.3 mol dm^{-3} $ZnCl_2$ in 1 mol dm^{-3} MSA. Although not included here, experiments have also been conducted in solutions containing more $ZnCl_2$ (i.e., 1.0 mol dm^{-3} ZnMSA/0.5 mol dm^{-3} $ZnCl_2$ in 1 mol dm^{-3} MSA), but little further change in the electrode response from that obtained in 1.2 mol dm^{-3} ZnMSA/0.3 mol dm^{-3}) $ZnCl_2$ in 1 mol dm^{-3} MSA was observed. Thus, no further experiments in electrolytes containing more than 0.3 mol dm^{-3} $ZnCl_2$ have been conducted.

3.2. Effect of mixed methanesulfonate/sulfate electrolyte

Figure 3 shows cyclic voltammograms of the Zn/Zn(II) system in different mixed methanesulfonate/sulfate electrolytes and the corresponding pure electrolytes containing a total dissolved Zn(II) concentration of 0.7 mol dm^{-3} in

0.2 mol dm^{-3} MSA (Table 1). As Table 2 shows, the presence of sulfate ions has a different effect from that of chloride by leading to a slight increase in E_{nu} ($\sim$ 20 mV), reflecting of a larger overpotential and more difficult onset of zinc electrodeposition in mixed methanesulfonate/sulfate electrolyte compared to the pure ZnMSA electrolyte. Although the charge efficiencies are comparable in both pure and mixed electrolytes, the current density throughout the cathodic portion of the scan and the anodic charge reflecting the amount of zinc deposited are lower in the sulfate-containing solutions. Thus, although a mixed methanesulfonate/sulfate electrolyte would have some benefits in an undivided zinc/cerium RFB since it enhances the Ce(IV) solubility [10], our results show that the kinetics of the Zn/Zn(II) redox reaction will suffer.

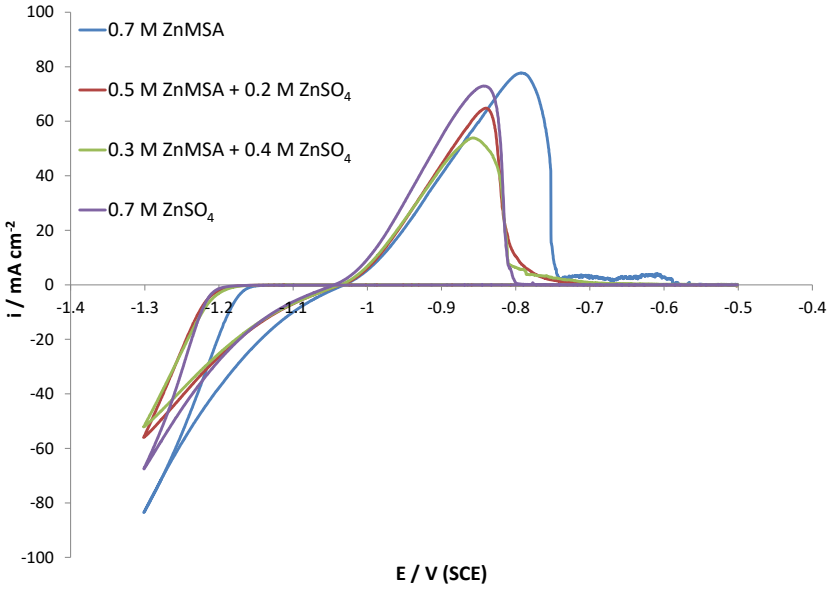

Figure 3: Cyclic voltammograms on a glassy carbon electrode ($\sim$ 0.071 cm^2) in different mixed methanesulfonate/sulfate media with 0.2 mol dm^{-3} MSA base electrolyte at 25°C and a scan rate of 20 mV s^{-1}.

The CVs in these previous two sections clearly show that the addition of chloride ions to the MSA base electrolyte leads to larger cathodic and anodic

current densities and more zinc deposition compared to that obtained in the pure MSA and sulfate-containing electrolytes. Also, the effect of the anions on the overpotential for zinc deposition on glassy carbon electrode increases in the following order: $Cl^- < CH_3SO_3^- < SO_4^-$. As previously mentioned, chloride ions have been shown to enhance the electrodeposition of other metals as well. One proposed mechanism for this effect is the bridging effect of chloride ions [30,39]. In this mechanism, the chloride ions adsorb on the electrode substrate and facilitate the electron transfer between the metal cations and the electrode by forming bridges between them [30].

Another important factor is the strength of the interaction between Zn(II) and the various ligands present which must be overcome in order to discharge and deposit the metal. Consequently, the more stable a zinc ion-pair or complex is, the slower should be the rate of zinc nucleation and deposition. One measure of the strength of such an interaction is the magnitude of the stability constant for its formation. The stability constant for the formation of the $ZnCl^+$ complex at zero ionic strength is $10^{0.96}$ [40]. On the other hand, the stability constant for the formation of $ZnSO_4$ complex at zero ionic strength is $10^{2.38}$ [40]. Based on this criterion, it should be easier to discharge Zn(II) and deposit metal in the former than the latter electrolyte. This can explain the lower overpotential for Zn(II) reduction in a mixed methanesulfonate/chloride bath compared to a mixed methanesulfonate/sulfate electrolyte. No data were found in the literature for the stability constant of zinc methanesulfonate complexes. However, it has been reported that methanesulfonate ions are stronger complexing agents than chloride for other metals such as lead and cadmium [41]. Additionally, a previous study on nickel deposition has shown that the overpotential for Ni(II) reduction increases in the sequence $ClO_4^- < CH_3SO_3^- < SO_4^-$, which leads to the expectation that nickel-methanesulfonate complexes are less thermodynamically favored than nickel-sulfate complexes and more than those containing chloride [42]. In this study, we have found a similar trend in the overpotential for Zn(II) reduction and thus propose that the stability of zinc-methanesulfonate complexes is also higher than that of zinc-chloride complexes, leading to the

mixed methanesulfonate/chloride bath being the most favorable electrolyte for deposition.

3.3. Determination of exchange current density

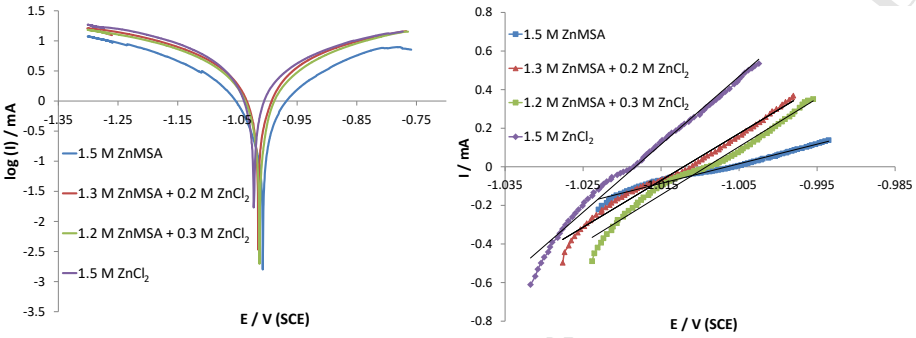

(a) (b)

Figure 4: (a) Semi-log plot of current versus potential on a glassy carbon electrode (~ 0.071 cm^2) immersed in different mixed methanesulfonate/chloride media obtained at a scan rate of 2 $mV\,s^{-1}$. (b) Linear polarization measurements for zinc on a glassy carbon electrode obtained at a scan rate of 0.167 $mV\,s^{-1}$.

Our results in Table 2 suggest that the addition of chloride enhances the kinetics of the zinc redox reaction. Thus, we have conducted polarization experiments to find the change in the values of exchange current densities upon addition of chloride to the solution. Figure 4a is obtained by scanning the potential at a sweep rate of 2 $mV\,s^{-1}$ up to 0.250 V in both directions from the open circuit potential for each electrolyte shown in Table 3. The Butler-Volmer equation (Eqn (1)) has been fitted to the experimental data to obtain the exchange current density (i_0), β_a and β_c. A non-linear least-square method that makes use of the trust region reflective algorithm (TRF) has been used to do this fitting.

$$i = i_0 \left(\exp\left(\frac{2.3(E - E_{ocp})}{\beta_a}\right) - \exp\left(-\frac{2.3(E - E_{ocp})}{\beta_c}\right) \right) \quad (1)$$

As Table 3 shows, the exchange current density increases from 11.3×10^{-3} A cm^{-2} to 21.7×10^{-3} A cm^{-2} upon addition of 0.2 mol dm^{-3} $ZnCl_2$ and rises to 24.0×10^{-3} A cm^{-2} when 0.3 mol dm^{-3} $ZnCl_2$ is added. The highest exchange current density was found for the pure $ZnCl_2$ solution. These values are in the same range (10^{-3} A cm^{-2}) as the reported values for zinc redox reaction in pure chloride and MSA electrolytes [43,44]. It should be noted that as Table 3 shows, the β_c and β_a extracted from Figure 4a are all larger than the expected value for a two-electron transfer (60 mV decade^{-1}). However, they are in agreement with the values reported in previous studies on zinc deposition and dissolution reaction in pure MSA solutions [45].

For the linear polarization technique, a potential sweep rate of 0.117 mV s^{-1} was used and the potentials were limited to 0.010 V from the open circuit potential. In this range of overpotential, current changes linearly with voltage (Figure 4b). Similar to the results found from fitting the Butler-Volmer equation to the experimental data, the exchange current densities increase as the chloride concentration is raised. The difference between the values obtained by these two methods has also been reported in a previous study on zinc redox reaction in pure MSA electrolyte [45] and is attributed to the occurrence of hydrogen evolution reaction particularly at higher overpotentials.

Table 3: Open circuit potential (E_{ocp}), $-\beta_c$ and β_a along with the exchange current density (i_0) calculated from fitting the Butler-Volmer equation to experimental data and use of the linear polarization method.

Compositon (mol dm^{-3})	Fitting of Butler-Volmer Equation				Linear polarization
	E_{ocp} (V)	$-\beta_c$ (mV decade^{-1})	β_a (mV decade^{-1})	i_0 mA cm^{-2}	i_0 mA cm^{-2}
1.5 ZnMSA	-1.008	177	170	11.3	5.4
1.3 ZnMSA + 0.2 $ZnCl_2$	-1.011	170	170	21.7	12.7
1.2 ZnMSA + 0.3 $ZnCl_2$	-1.014	200	200	24.0	15.2
1.5 $ZnCl_2$	-1.023	181	200	27.0	21.9

3.4. Determination of diffusion coefficients for Zn(II)

In order to study the possible effect of chloride and sulfate ions on the transport properties of Zn(II), we conducted a series of linear sweep voltammetry experiments on a rotating GC electrode in various Zn(II)-containing solutions over the potential range where zinc deposition occurs. As mentioned previously, zinc deposition is accompanied by HER in all the electrolytes considered so far in this study due to their acidic conditions. This greatly complicates the accurate determination of the diffusion coefficient of Zn(II) using the Levich equation since the limiting current plateaus for its reduction do not clearly appear in the linear sweep voltammograms obtained in these solutions. Consequently, we have chosen to measure the Zn(II) diffusion coefficients in electrolytes that contain lower Zn(II) concentrations and are less acidic to ensure that it is possible for the measured current to be controlled by diffusion of Zn(II) alone. Table 4 shows the composition of the electrolytes used for estimation of the diffusion coefficients. The pure MSA and mixed electrolyte solutions are adjusted to pH 4 by adding 0.5 $\mathrm{mol\,dm^{-3}}$ NaMSA and the appropriate amount of MSA. Solutions with pure chloride and sulfate ions have also been characterized for comparison. 0.5 $\mathrm{mol\,dm^{-3}}$ NaCl or Na_2SO_4 are added to these solutions and the pH is adjusted to 4 using the appropriate amount of HCl or H_2SO_4.

Figure 5a shows the cyclic voltammograms obtained in the different mixed methanesulfonate/chloride electrolytes containing a total of 0.02 $\mathrm{mol\,dm^{-3}}$ Zn(II) (Table 4) at 25°C on a static glassy carbon electrode. In these experiments, the potential is swept first from -0.8 to -1.4 V *vs* SCE and then reversed back to -0.8 V at a scan rate of 20 $\mathrm{mV\,s^{-1}}$. Similar to that observed previously in the more concentrated solutions, the addition of chloride shifts the E_{nu} to more positive values and increases the current density and amount of zinc deposited. As reported previously [6], the limiting current density i_L is an important factor in the charge/discharge of RFBs. Operation at current densities higher than i_L leads to excessive hydrogen evolution and hence a lower charge efficiency when the battery is being re-charged. Figure 5b shows the electrode responses obtained at 1600 rpm for the same compositions shown in Figure 5a. As can

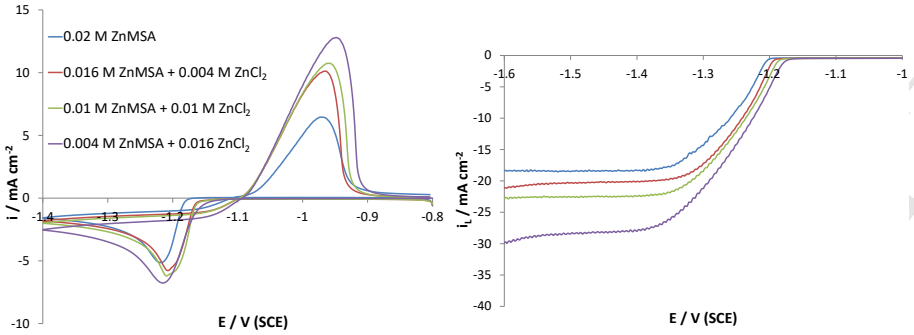

(a) (b)

Figure 5: (a) Cyclic voltammograms on a glassy carbon electrode ($\sim$ 0.071 cm^2) immersed in different mixed methanesulfonate/chloride media at 25°C obtained at a scan rate of 20 $mV\,s^{-1}$. (b) Comparison of linear sweep voltammograms for RDE rotating at 1600 rpm for the same compositions shown in Figure 5a. Scan rate = 20 $mV\,s^{-1}$.

be seen, these plots show that the limiting current density for Zn(II) reduction is increased significantly by the presence of chloride (e.g., an increase from $\sim$ -18 $mA\,cm^{-2}$ to $\sim$ -29 $mA\,cm^{-2}$ as the $ZnCl_2$ concentration is raised from 0 to 0.016 $mol\,dm^{-3}$) despite the fact that the total amount of Zn(II) in solution remains unchanged. A similar trend is observed at the other rotation speeds.

Linear sweep experiments over the potential range from -1.0 V to -1.9 V *vs* SCE at a scan rate of 20 $mV\,s^{-1}$ on an RDE operating at rotation speeds of 400, 900, 1600, 2500 and 3600 rpm have been conducted for each composition given in Table 4. Figure 6a shows an example of the set of linear sweep voltammograms obtained in one of the solutions (0.01 $mol\,dm^{-3}$ ZnMSA/0.01 $mol\,dm^{-3}$ $ZnCl_2$ in 0.5 $mol\,dm^{-3}$ NaMSA) at pH 4. The current density for the mass transport-limited reaction of an electroactive species at a rotating disk electrode is described by the Levich equation [46]

$$i_L = 0.620nFD^{2/3}\omega^{1/2}v^{-1/6}c \qquad (2)$$

where n is the number of transferred electrons (2 in this case), F is the Faraday constant, D is the diffusion coefficient, ω is the rotation speed expressed in

rad s^{-1}, v is the kinematic viscosity and c is the concentration of the electroactive species. Figure 6b shows a plot of i_L versus $w^{1/2}$ according to the Levich equation for the solution considered in Figure 6a. As predicted by the Levich equation, the plot is linear and passes through the origin. Although not included here, similar results are obtained for the other solutions. Table 4 shows the diffusion coefficients obtained from the slope of the best straight line plot for various electrolytes. Also included in the table are the corresponding kinematic viscosities measured directly in our study. The dimensionless Schmidt number which is the ratio of the dynamic viscosity of the electrolyte to the diffusion coefficient is also included in this table. This number is important for characterizing the flow conditions and is relevant to the design of redox flow batteries. The diffusion coefficient of zinc in pure methanesulfonate, sulfate and chloride solutions is found to be 4.6×10^{-6} $cm^2\,s^{-1}$, 4.4×10^{-6} $cm^2\,s^{-1}$, 8.6×10^{-6} $cm^2\,s^{-1}$, respectively. The values obtained in the sulfate- and chloride-only solutions are in good agreement with those reported previously [18,22]. In a previous study [10] the diffusion coefficient of Zn(II) in a pure methanesulfonate solution was found to have a somewhat higher value of 7.5×10^{-6} $cm^2\,s^{-1}$ than that reported here although it should be noted that this earlier measurement was conducted in a solution with a different concentration (0.01 mol dm^{-3} ZnMSA in 0.5 mol dm^{-3} NaMSA). Also, in this earlier study, the kinematic viscosity of the electrolyte was not measured and instead a value from the literature was assumed for the purpose of estimating diffusion coefficient.

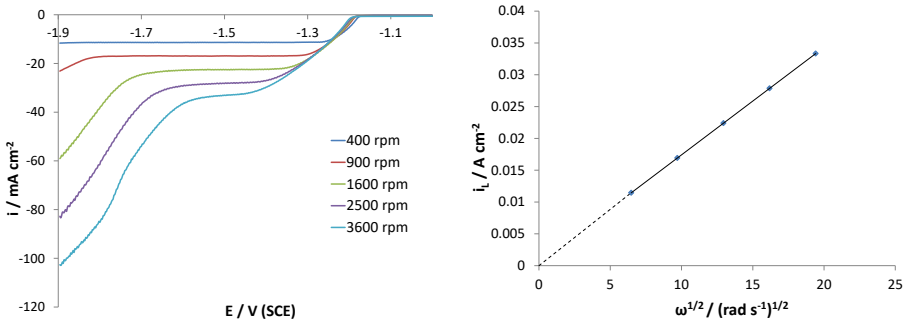

(a) (b)

Figure 6: (a) Linear sweep voltammograms for Zn(II) reduction on a glassy carbon electrode ($\sim$ 0.071 cm^2) obtained at a scan rate of 20 $mV\,s^{-1}$ and different rotation speeds in 0.01 $mol\,dm^{-3}$ ZnMSA/0.01 $mol\,dm^{-3}$ $ZnCl_2$ and 0.5 $mol\,dm^{-3}$ NaMSA at pH 4. (b) Plot of limiting current density versus $\omega^{1/2}$ according to the Levich equation obtained in the same solution.

Table 4: Kinematic viscosity, diffusion coefficient and Schmidt number measured in various mixed electrolytes.

Composition ($mol\,dm^{-3}$)	Kinematic viscosity (10^{-2} $cm^2\,s^{-1}$)	Diffusion coefficient (10^{-6} $cm^2\,s^{-1}$)	Schmidt number
0.02 ZnMSA	1.064	4.6	0.23
0.016 ZnMSA + 0.004 $ZnCl_2$	1.092	5.3	0.21
0.01 ZnMSA + 0.01 $ZnCl_2$	1.076	6.0	0.18
0.004 ZnMSA + 0.016 $ZnCl_2$	1.088	8.3	0.13
0.02 $ZnCl_2$	1.012	8.5	0.12
0.016 ZnMSA + 0.004 $ZnSO_4$	1.052	4.4	0.24
0.01 ZnMSA + 0.01 $ZnSO_4$	1.064	5.1	0.21
0.004 ZnMSA + 0.016 $ZnSO_4$	1.052	5.7	0.18
0.02 $ZnSO_4$	1.360	4.4	0.31

** pH of all solutions adjusted to 4 through additions of 0.5 $mol\,dm^{-3}$ NaMSA to the methanesulfonate solutions and 0.5 $mol\,dm^{-3}$ NaCl or Na_2SO_4 to the chloride- or sulfate-only solutions.

435 The results in Table 4 show that as more ZnMSA is replaced with $ZnCl_2$
436 in the electrolyte, the diffusion coefficient increases and approaches the value

obtained in a solution containing $ZnCl_2$ alone. On the other hand, the diffusion coefficients in the mixed methanesulfonate/sulfate media differ only slightly from the values observed in the sulfate-only or methanesulfonate-only electrolytes.

3.5. Effect of operating parameters in mixed methanesulfonate/chloride electrolyte

3.5.1. Effect of temperature

Temperature is one of the important operating variables for redox flow batteries. Whereas the proposed undivided zinc-cerium RFB has been operated at room temperature [15], higher temperatures (40°C-60°C) have been used for the divided zinc-cerium RFBs [5]. Thus, the effect of temperature on the Zn/Zn(II) system in mixed methanesulfonate/chloride media is compared to that in the MSA-only electrolyte for compositions used on the zinc negative half-cell side of a divided zinc-cerium RFB.

Figure 7 shows the cyclic voltammograms obtained in solutions containing 1.2 $\mathrm{mol\,dm^{-3}}$ ZnMSA/0.3 $\mathrm{mol\,dm^{-3}}$ $ZnCl_2$ in 1 $\mathrm{mol\,dm^{-3}}$ MSA compared to those obtained in the MSA-only electrolyte (1.5 $\mathrm{mol\,dm^{-3}}$ ZnMSA in 1 $\mathrm{mol\,dm^{-3}}$ MSA) at 25, 35 and 45°C. The values of E_{nu}, NOP , I_{ac} and Q_{an} determined from these plots for both electrolytes at the three temperatures are summarized in Table 5. These data show that an increase in temperature leads to a positive shift of E_{nu} in both electrolytes, but has much less effect in the mixed methanesulfonate/chloride solution. An increase of E_{nu} is expected from both thermodynamic and kinetic points of view. The electrode potential for Zn/Zn(II) increases with temperature according to the Nernst equation, while the rate of formation of metal clusters large enough to ensure spontaneous growth should also rise with temperature as given in classical nucleation theory and the Volmer-Weber equation [47]. The data in Table 6 indicate that an increase in temperature causes the amount of zinc deposited during the scan to rise and NOP to decline in both electrolytes. However, they also reveal that the rise in E_{nu} and the amount of zinc deposited during the cathodic scan are significantly

higher and NOP is always smaller in the mixed system than in the MSA-only electrolyte at each temperature. At 45 °C, the amount of deposited zinc is 50% higher and the NOP is 86% lower when the mixed electrolyte is used than when MSA-only media are used. Although the NOP tends to decrease in magnitude with temperature, the value for the pure MSA electrolyte at 45°C is 93 mV, which is still higher than the value of 50 mV in the methanesulfonate/chloride electrolyte. This highlights the important role that chloride plays in facilitating zinc deposition. In fact, the improved kinetics achieved at 45°C in the pure MSA electrolyte is already observed in the methanesulfonate/chloride solution at room temperature.

To accurately determine the effect of temperature on the charge efficiency of Zn deposition, we also have conducted experiments in which the GC electrode immersed in the solutions of interest is galvanostatically polarized at 25 $\mathrm{mA\,cm^{-2}}$ first in the cathodic direction for 30 s and then with the same magnitude of current in the anodic direction. Figure 8 shows the resulting response of the electrode potential over this time obtained in the mixed and the MSA-only electrolytes at the three temperatures, while Table 6 summarizes the corresponding data for these experiments. The transient curves for both electrolytes show that the electrode is immediately depolarized at the onset of the cathodic polarization until a plateau is reached. This is not surprising given that the nucleation overpotential for zinc deposition should decrease as the zinc deposit begins to build on the GC substrate and is consistent with the features of the cyclic voltammograms shown in Figure 7 and Table 5. When the polarity is reversed and anodic current is applied, the response of the system is extremely rapid and a plateau is reached almost immediately in both electrolytes regardless of the temperature. This continues for $\sim$ 25–30 s of anodic polarization until all of the zinc metal deposited during cathodic polarization has been stripped, at which point the potential increases very sharply in the positive direction and the experiment is terminated. The curves in Figure 8 clearly show that temperature has a much smaller effect on the electrode response obtained in the mixed electrolyte than in the MSA-only electrolyte, which is consistent

with the effects on E_{nu} and NOP observed in the CV scans in Figure 7 and listed in Table 5. The curves in Figure 8 are relevant to battery applications in that they give the response of the negative Zn electrode that might be expected during a short charge/discharge cycle of a system operating at a given current density. Comparison of the curves reveals a number of benefits of using the mixed methanesulfonate/chloride electrolyte rather than the pure MSA electrolyte. The electrode potential reaches a plateau level where the rate of growth or re-dissolution of zinc is constant almost immediately during both the cathodic and anodic (charge and discharge) portions of the cycle at the three temperatures. On the other hand, the electrode potential never levels off to a constant value by the end of the 30–s duration of cathodic polarization in the MSA-only solution at any temperature. Once the polarity of the current is reversed in the anodic direction, the polarization of the electrode continues to gradually rise until the Zn deposit has completely dissolved from the electrode when carried out in the MSA-only electrolyte, whereas the electrode is able to maintain an almost constant potential until the Zn deposit has deposit has been removed in the case of the mixed electrolyte.

The operation of a rechargeable battery is most efficient when the polarization of both electrodes is as low as possible during both charge and discharge. Thus, it is desirable for the electrode potential to be as positive as possible during charge when Zn(II) reduction occurs and as negative as possible during discharge when Zn oxidation occurs. The result will be the smallest change in the electrode potential during the course of a complete charge/discharge cycle. When viewed this way, a comparison of the transient curves in Figure 8 clearly shows that with the exception of cathodic polarization at 45°C better performance is achieved in the mixed electrolyte than the pure MSA system.

Since the magnitude of the applied current is the same during both stages of these experiments, the charge efficiency for Zn deposition can simply be obtained from the data in Figure 8 from the ratio of the elapsed time required to completely strip the Zn deposit from the substrate during the anodic polarization to the period allowed for cathodic polarization (30 s in this case). The

sharp rise in the electrode potential observed when the Zn deposit has been removed makes the determination of the charge efficiency from these plots very straightforward. Although the solution conductivity and voltage efficiency both increase as temperature is raised, the charge efficiency for Zn deposition in pure MSA electrolyte has been previously shown to decrease due to the higher rate of the HER [6]. The effect of temperature in the case of mixed electrolytes has not previously been reported. The results in Table 6 not only confirm that temperature has a similar effect in the MSA-only electrolyte investigated in our study but that this effect extends to the mixed electrolyte as well. Thus, the larger cathodic current density observed during the scans in Figure 7 as the temperature is raised in both solutions is due to the higher rates of both zinc deposition and hydrogen evolution.

Nevertheless, for the most part, our results clearly show the enhanced performance of the Zn/Zn(II) reaction in mixed-electrolyte media in terms of higher voltage and charge efficiency compared to that achieved in MSA-only electrolyte at each temperature, which leads to a significantly larger energy efficiency. Even with the decrease in the charge efficiency with temperature due to the higher rate of the HER, the energy efficiency at 45°C in the mixed media is still greater than the energy efficiency achieved at room temperature in the pure MSA electrolyte. This observation is particularly important for divided zinc-cerium RFBs that are operated at higher temperatures to enhance the kinetics of the Ce(III)/Ce(IV) reaction. By using the mixed methanesulfonate/chloride electrolyte, the Zn/Zn(II) half-cell performance at 45°C is superior in terms of E_{nu}, NOP, voltage and charge efficiency to that achieved in pure MSA electrolytes at room temperature.

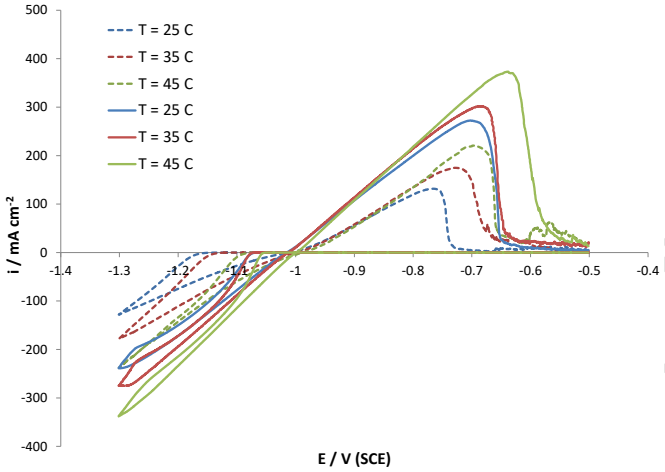

Figure 7: Cyclic voltammograms obtained on a glassy carbon electrode ($\sim$ 0.071 cm^2) in mixed methanesulfonate/chloride media (solid line) and MSA-only electrolyte (dashed line) at three different temperatures.

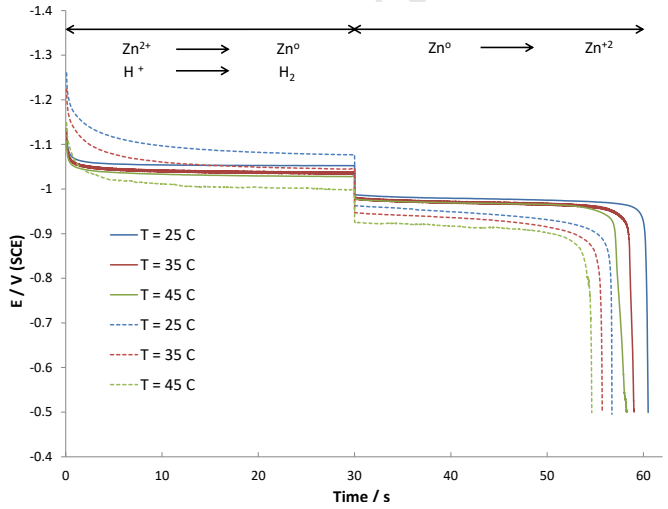

Figure 8: Variation of electrode potential with time during galvanostatic cathodic and anodic polarization of glassy carbon electrode ($\sim$ 0.071 cm^2) at 25 mA cm^{-2} in mixed methanesulfonate/chloride media (solid line) and MSA-only electrolyte (dashed line) at three different temperatures.

Table 5: Effect of temperature, MSA and zinc concentration on E_{nu}, NOP, I_{ac} and Q_{an} of zinc deposition in mixed methanesulfonate/chloride and MSA-only electrolytes. The corresponding figures and compositions for each temperature, MSA and zinc concentration are explained in sections 3.4.1, 3.4.2 and 3.4.3, respectively.

Operating parameter	E_{nu} (V)		-NOP (mV)		I_{ac} (mA cm^{-2})		Q_{an} (mA s)	
	MSA -only	Mixed electrolyte	MSA -only	Mixed electrolyte	MSA -only	Mixed electrolyte	MSA -only	Mixed electrolyte
Temperature (°C)								
25	-1.15	-1.07	140	50	131.6	272.4	73.4	204.8
35	-1.12	-1.07	122	50	174.8	301.9	111.9	230.0
45	-1.08	-1.05	93	50	220.7	373.2	152.9	309.4
MSA concentration (mol dm^{-3})								
0.2	-1.15	-1.11	120	80	77.7	123.0	42.9	67.4
0.5	-1.15	-1.12	130	80	113.7	147.0	61.1	85.0
1.0	-1.16	-1.14	150	90	125.1	208.8	64.9	90.0
Zinc concentration (mol dm^{-3})								
0.7	-1.15	-1.11	120	80	77.7	123.0	42.9	67.4
1.0	-1.14	-1.10	120	70	98.0	158.6	57.9	118.7
1.5	-1.13	-1.06	120	50	118.8	213.1	74.5	174.7

Table 6: Half-cell efficiencies of zinc deposition and dissolution of zinc in mixed MSA/chloride electrolyte and MSA-only electrolytes. The corresponding figures and compositions for each temperature, MSA, zinc concentration and current density are explained in sections 3.4.1, 3.4.2, 3.4.3 and 3.4.4 respectively.

Operating parameter	VE%		CE%		EE%	
	MSA -only	Mixed	MSA -only	Mixed	MSA -only	Mixed
Temperature (°C)						
25	87.7	92.6	86.0	97.3	75.4	90.1
35	89.2	93.0	82.3	94.3	73.5	87.7
45	91.2	93.9	77.3	86.9	70.6	80.6
MSA concentration ($\mathrm{mol\,dm^{-3}}$)						
0.2	81.1	90.9	77.0	95.0	62.4	86.4
0.5	82.9	90.6	76.0	91.7	63.0	83.5
1.0	83.9	93.6	71.3	88.7	59.8	83.0
Zinc concentration ($\mathrm{mol\,dm^{-3}}$)						
0.7	81.1	90.9	77.0	95.0	62.4	86.4
1.0	84.6	91.1	82.3	96.7	69.6	88.1
1.5	86.2	92.0	87.3	97.7	75.3	89.9
Current density ($\mathrm{mA\,cm^{-2}}$)						
5	95.5	97.1	80.0	87.7	76.4	83.1
25	87.7	92.6	86.0	97.3	75.4	90.1
35	84.5	91.0	86.7	92.7	73.2	84.3
45	80.4	87.3	85.0	93.7	68.3	81.8
55	77.6	86.7	84.3	92.3	65.4	80.9

3.5.2. Effect of methanesulfonic acid concentration

Cyclic voltammograms showing the effect of the addition of different amounts of methanesulfonic acid to a mixed methanesulfonic acid/chloride solution (0.5 $\mathrm{mol\,dm^{-3}}$ ZnMSA/0.2 $\mathrm{mol\,dm^{-3}}$ $ZnCl_2$) and to a pure MSA electrolyte (0.7 $\mathrm{mol\,dm^{-3}}$ ZnMSA) are presented in Figure 9. The corresponding data obtained from these plots are given in Table 5. The data show that the nucleation potential is largely independent of the MSA concentration and shifts only slightly in the negative direction as the MSA concentration is increased. The NOP

is affected more strongly, particularly in the MSA-only solution where it rises from 120 mV to 150 mV as the MSA level is increased from 0.2 mol dm^{-3} to 1.0 mol dm^{-3}. As can be seen, the cathodic current density and amount of zinc deposited during the scans increase in both electrolytes (pure and mixed) when the concentration of the base MSA electrolyte is raised. However, these values always remain higher for the case of the mixed electrolyte. In addition, the onset potential for zinc deposition is more positive and the NOP is significantly lower in the mixed electrolyte than in the MSA-only system.

Figure 10 shows the effect of MSA concentration on the electrode potential during the course of galvanostatic cathodic and anodic polarization of the GC electrode at 25 mA cm^{-2} in the mixed and pure MSA electrolytes, while Table 6 presents the voltage, charge and energy efficiencies obtained from these experiments. A comparison of these transients shows the clear superiority of the system performance when the mixed electrolyte is used in terms of the lower extent of polarization required to sustain the applied current during both the cathodic and anodic stages, faster attainment of plateau and charge efficiency of Zn deposition.

When the effect of MSA level in each electrolyte is considered, these data reveal that a rise in its concentration leads to more metal deposition, but favors the HER even more. This effect is perfectly understandable given that MSA is the source of H^+ ions. It should be noted that although the charge efficiency decreases as the MSA concentration increases in both solutions, the charge efficiency in the mixed methanesulfonate/chloride media remains higher than in the MSA-only electrolyte at each MSA concentration. Furthermore, although the energy efficiency of zinc deposition decreases with increasing MSA concentrations due to reduction in the charge efficiency, the energy efficiency in the mixed media containing 1.0 mol dm^{-3} MSA is significantly higher than that in pure MSA electrolyte with 0.2 mol dm^{-3} base MSA. Thus, by employing the mixed electrolyte system, it is possible to operate the cell over a wider range of MSA concentrations without the Zn/Zn(II) reaction being negatively affected. Again, this advantage of the mixed electrolyte is particularly important for an undivi-

ded zinc-cerium RFB where high MSA concentrations are required to dissolve the Ce(IV). It has been reported that the optimum composition from the point of view of the solubility of cerium species is approximately 0.8 mol dm^{-3} Ce(III) ion in 4.0 mol dm^{-3} MSA [7]. However, at this high MSA concentration, the HER becomes dominant on the zinc side. Thus, for an undivided zinc-cerium RFB, a compromise must be made between a lower hydrogen evolution rate at the zinc side and higher solubility of cerium in the electrolyte. This normally requires that the battery be operated at low MSA concentrations and consequently only at a low Ce(III) concentration ($\sim$ 0.2 mol dm^{-3}) [15]. This leads to a low energy density of 11 W h L^{-1} for an undivided system. Hence, it would be beneficial to achieve higher charge efficiencies for zinc electrodeposition when the solution contains a higher MSA concentration and the battery can produce a higher energy density. As shown in this study, this is possible by using a mixed methanesulfonate/chloride electrolyte, which enables the charge and voltage efficiency for zinc deposition achieved in the presence of 1.0 mol dm^{-3} MSA to be better to that achieved when only 0.2 mol dm^{-3} MSA has been added.

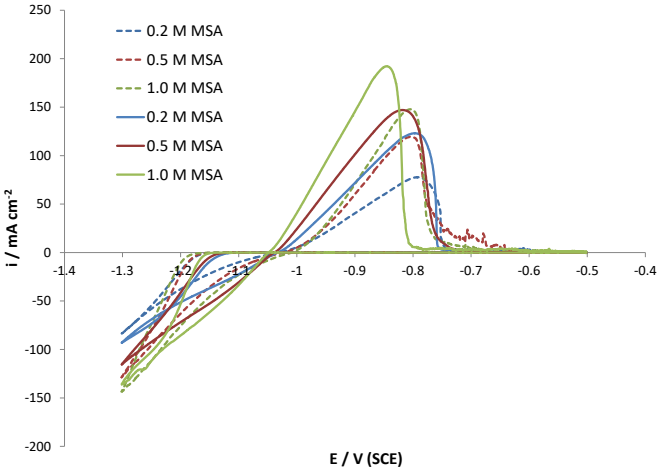

Figure 9: Cyclic voltammograms on a glassy carbon electrode ($\sim$ 0.071 cm^2) obtained in 0.5 $mol\,dm^{-3}$ ZnMSA/0.2 $mol\,dm^{-3}$ $ZnCl_2$ (solid line) and in 0.7 $mol\,dm^{-3}$ electrolyte (dashed line) containing three different MSA base concentrations (0.2, 0.5 and 1.0 $mol\,dm^{-3}$).

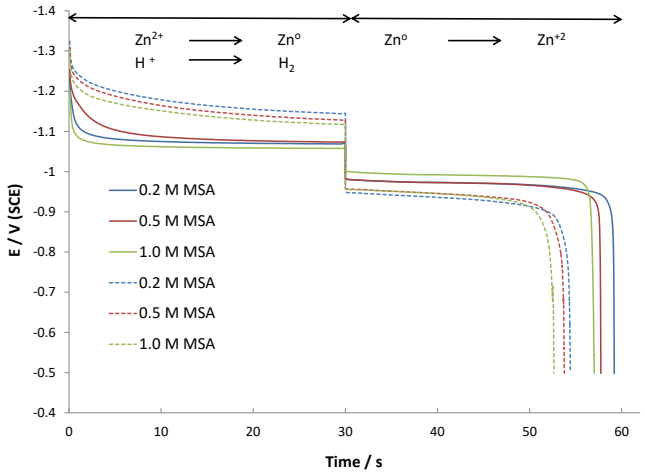

Figure 10: Variation of electrode potential with time during galvanostatic cathodic and anodic polarization of glassy carbon electrode ($\sim$ 0.071 cm^2) at 25 $mA\,cm^{-2}$ in 0.5 $mol\,dm^{-3}$ ZnMSA/0.2 $mol\,dm^{-3}$ $ZnCl_2$ (solid line) and in 0.7 $mol\,dm^{-3}$ electrolyte (dashed line) containing three different MSA base concentrations (0.2, 0.5 and 1.0 $mol\,dm^{-3}$).

3.5.3. *Effect of zinc ion concentration in mixed methanesulfonate/chloride media*

In order to investigate the effect of the Zn(II) concentration on the Zn/Zn(II) system, cyclic voltammograms have been obtained in each of the electrolytes listed in Table 4. In this series of experiments, the total Zn(II) concentration in the mixed electrolyte is increased from 0.7 $\mathrm{mol\,dm^{-3}}$ to 1.0 $\mathrm{mol\,dm^{-3}}$ and 1.5 $\mathrm{mol\,dm^{-3}}$, while the molar ratio of methanesulfonate ions to chloride ions is kept fixed at 5:2. Three solutions with 0.7 $\mathrm{mol\,dm^{-3}}$, 1.0 $\mathrm{mol\,dm^{-3}}$ and 1.5 $\mathrm{mol\,dm^{-3}}$ Zn(II), but in MSA-only electrolytes, are also investigated for comparison purposes. Also, 0.2 $\mathrm{mol\,dm^{-3}}$ MSA has been added to each of these mixed and pure solutions.

Not surprisingly, the cathodic and anodic current density, cumulative charges over the course of the scans of Zn deposition increase as the Zn(II) concentration rises in both electrolytes (Table 5). Also, this change causes the nucleation potential to become more positive. More interesting is the comparison of the effect of the Zn(II) concentration in the two types of electrolytes. E_{nu} is more positive, NOP is smaller, while the amount of metal deposited is larger at each Zn(II) concentration when the process is conducted in the mixed methanesulfonate/chloride electrolyte than in the MSA-only electrolyte. Furthermore, the positive effect of the Zn(II) concentration on the amount of metal deposited is significantly larger in the mixed methanesulfonate/chloride electrolyte than in the MSA-only electrolyte.

Figure 12 shows the effect of the Zn(II) concentration on the electrode potential during the course of galvanostatic cathodic polarization and anodic polarization at 25 $\mathrm{mA\,cm^{-2}}$ in the mixed and pure MSA electrolytes. Obviously, zinc deposition becomes increasingly favored over the HER by the increase in the Zn(II) concentration. Previous studies also found that the charge efficiency increases from 78% in 0.5 $\mathrm{mol\,dm^{-3}}$ Zn(II) to 92% in 2.0 $\mathrm{mol\,dm^{-3}}$ Zn(II) when 1.5 $\mathrm{mol\,dm^{-3}}$ pure MSA electrolyte is used [6]. The transients in Figure 12 show that this leads to less polarization during reduction in both electrolytes

although the effect of the Zn(II) concentration is larger in the MSA-only case. On the other hand, the Zn(II) concentration has no effect on the electrode potential in both solutions as Zn is being oxidized during the anodic polarization. Comparison of the transients also reveals once again the benefits of using the mixed electrolyte over that of the pure MSA electrolyte at each of the Zn(II) levels (less polarization throughout both stages of the cycle, faster attainment of plateau and higher charge efficiency of Zn deposition).

The data in Table 6 reveal that at each Zn(II) concentration, the charge and voltage efficiencies are significantly higher in the mixed electrolyte than in the pure MSA solution. It is desirable to use a higher Zn(II) concentration since this reduces the likelihood that mass transfer will affect battery performance at all states-of-charge and permits the battery to be charged at higher current densities. By using the mixed electrolyte rather than the MSA-only solution, it is possible to achieve a higher energy efficiency with lower nucleation overpotential at high Zn(II) concentrations.

Table 7: Different compositions used to study the effect of Zn(II) concentration in mixed methanesulfonate/chloride and pure MSA electrolytes that also contain 0.2 mol dm^{-3} MSA.

ZnMSA (mol dm^{-3})	$ZnCl_2$ (mol dm^{-3})
0.7	0
1.0	0
1.5	0
0.5	0.2
0.714	0.285
1.072	0.42

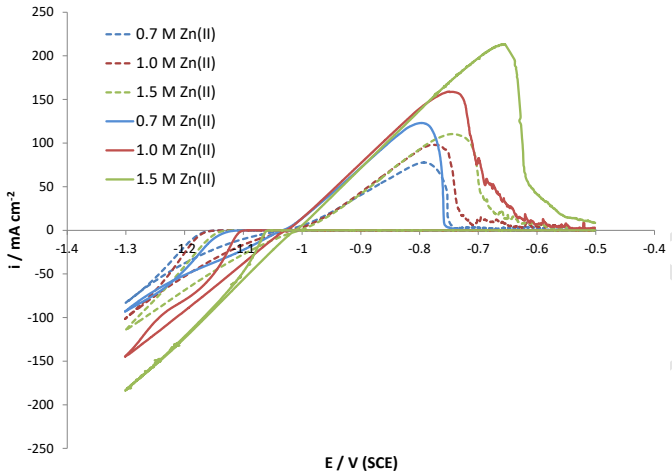

Figure 11: Cyclic voltammograms on a glassy carbon electrode ($\sim$ 0.071 cm^2) obtained in mixed methanesulfonate/chloride media (solid line) and MSA-only electrolyte (dashed line) containing 0.7, 1.0 and 1.5 mol dm^{-3} total Zn(II). The solution compositions are listed in Table 7.

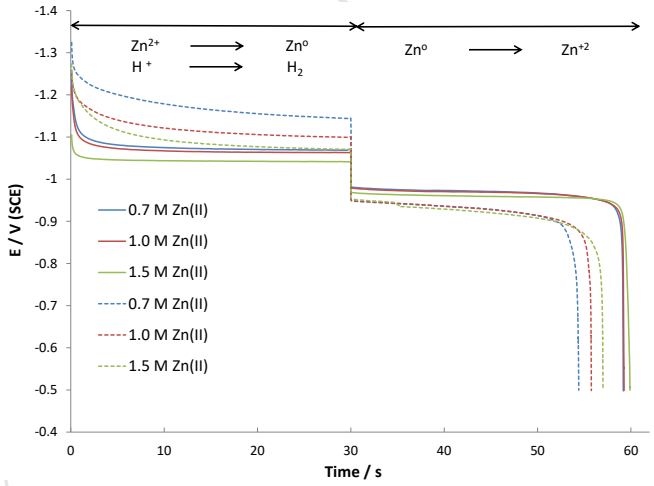

Figure 12: Variation of electrode potential with time during galvanostatic cathodic and anodic polarization of glassy carbon electrode ($\sim$ 0.071 cm^2) at 25 mA cm^{-2} in mixed methanesulfonate/chloride media (solid line) and MSA-only electrolyte (dashed line) containing 0.7, 1.0 and 1.5 mol dm^{-3} total Zn(II). The solution compositions are listed in Table 7.

3.5.4. Effect of current density

Figure 13 shows the effect of current density on the charge/discharge of the zinc redox reaction in solutions containing 1.2 mol dm^{-3} ZnMSA/0.3 mol dm^{-3} $ZnCl_2$ in 1 mol dm^{-3} MSA compared to those obtained in the MSA-only electrolyte (1.5 mol dm^{-3} ZnMSA in 1 mol dm^{-3} MSA). Similar to previous studies [6,18], higher energy efficiency is found at a moderate current density of 25 mA cm^{-2}. The corresponding data in Table 5 show that the voltage efficiency decreases in both types of electrolytes as the current density is increased. Although the VE% is very high at a low current density of 5 mA cm^{-2}, due to the high self-discharge of zinc, the resulting charge efficiency is the lowest. As the current density is raised above 25 mA cm^{-2}, the current efficiency slightly decreases but is generally independent of the applied current density, which is in agreement with previous literature [48]. The data in Table 6 reveal that regardless of the applied current density, the charge, voltage and the resulting energy efficiency are higher in the mixed electrolyte compared to the pure MSA media and the highest energy efficiency is obtained at a current density of 25 mA cm^{-2}.

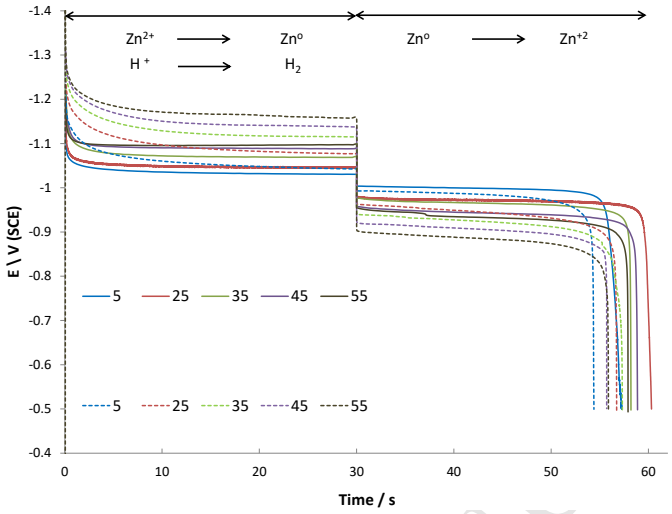

Figure 13: Variation of electrode potential with time during galvanostatic cathodic and anodic polarization of glassy carbon electrode ($\sim$ 0.071 cm^2) in mixed methanesulfonate/chloride media (solid line) and MSA-only electrolyte (dashed line) at different applied current densities. Current densities are in $mA\,cm^{-2}$.

3.6. Deposit morphology

Figure 14 shows the micrographs of zinc deposited from solutions containing 0.5 $mol\,dm^{-3}$ ZnMSA/0.2 $mol\,dm^{-3}$ $ZnCl_2$ compared to those obtained in the MSA-only electrolyte (0.7 $mol\,dm^{-3}$ ZnMSA). The base electrolyte was 0.2 $mol\,dm^{-3}$ MSA for both solutions. During deposition, the parallel hydrogen evolution reaction resulted in hydrogen bubbles covering many sites on the electrode surface. At some sites, these hydrogen bubbles could undercut and dislodge part of the zinc deposit. The poor surface adhesion of zinc onto glassy carbon electrode and the incomplete coverage of the GC electrode surface by zinc deposits have also been reported in a previous study on the comparison of different carbon materials for the negative side of the zinc-cerium redox flow batteries [45]. It should be noted that the use of carbon composite materials such as polyvinyl ester (PVE) and polyvinylidene difluoride (PVDF) largely solves these problems [45].

For both electrolytes, the deposited zinc is made up of hexagonal grains that

are randomly oriented on the electrode surface. This type of morphology for zinc deposits have also been reported in various previous studies [6,18,21]. By comparing the two images, it is clear that the addition of chloride has resulted in denser deposits with a more packed morphology. This is supported by our results in Table 5 which showed that regardless of the operating parameters, the anodic charge (which corresponds to the amount of deposited zinc) is significantly higher in mixed electrolytes than in the pure MSA media.

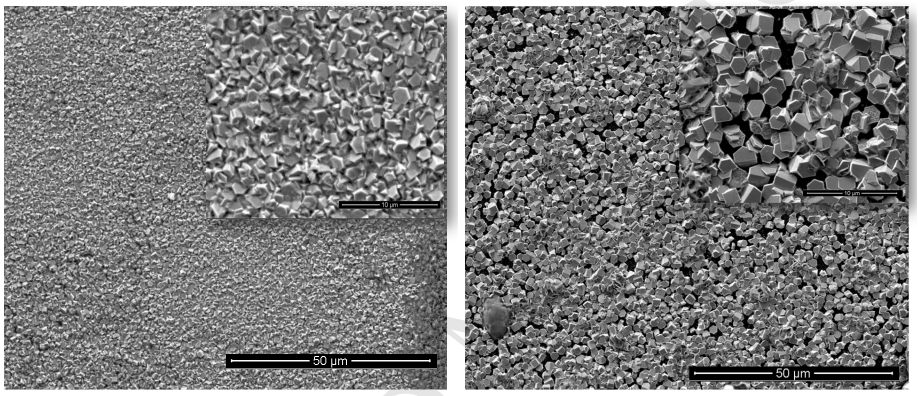

(a) (b)

Figure 14: The SEM images of zinc deposited from (a) 0.5 mol dm^{-3} ZnMSA/0.2 mol dm^{-3} $ZnCl_2$ and (b) 0.7 mol dm^{-3} ZnMSA onto glassy carbon plate ($\sim$ 0.25 cm^2). The deposition was done galvanostatically under constant current of 50 mA cm^{-2} for 1 minute.

4. Conclusions

- Cyclic voltammetry and linear polarization experiments show that the introduction of moderate concentrations of chloride ions (0.2 – 0.3 mol dm^{-3}) to MSA-based electrolytes leads to a significant increase in the rate and amount of Zn deposition, positive shift in the nucleation potential, reduction in the nucleation overpotential and enhanced exchange current densities.

- The addition of sulfate ions into the MSA-based electrolyte leads to a

lower rate of Zn deposition, slightly higher nucleation overpotential and similar charge efficiency to that attained in MSA-only electrolytes.

- The use of a mixed electrolyte has also been found to improve the transport properties of Zn(II). The diffusion coefficient of Zn(II) is found to be 6.0×10^{-6} $cm^2\,s^{-1}$ in 0.01 $mol\,dm^{-3}$ ZnMSA/0.01 $mol\,dm^{-3}$ $ZnCl_2$ compared to 4.6×10^{-6} $cm^2\,s^{-1}$ in 0.02 $mol\,dm^{-3}$ ZnMSA.

- Both potentiostatic and galvanostatic experiments conducted at 25, 35 and 45°C show that the rate, charge efficiency and voltage efficiency of Zn deposition are higher in the mixed methanesulfonate/chloride solution than in the MSA-only solution at each temperature.

- Although an increase in the base MSA concentration lowers the charge efficiency for Zn deposition in both pure and mixed MSA electrolytes, the use of a mixed methanesulfonate/chloride system leads to higher charge and voltage efficiency than in pure MSA electrolyte.

- The microghraph of zinc deposited from a mixed methansulfonate/chloride solution resulted in more packed morphology compared to the deposits from pure MSA electrolyte.

Since mixed methanesulfonate/chloride electrolytes have also been shown to increase the reversibility and kinetics of the Ce(III)/Ce(IV) half-cell reaction [11], it is also viable to use them as the common electrolytes in undivided zinc-cerium RFBs. However, before any further work on an undivided RFB is done, a thorough study on the effect of Ce(III) and Ce(IV) on the Zn/Zn(II) half-cell reaction is necessary and is the subject of our ongoing research.

Acknowledgement

The authors acknowledge the financial support of the Natural Sciences and Engineering Research Council of Canada (NSERC) through Discovery Grant 170912 which enabled this research to be carried out. They also express their

gratitude to Dr. Neil McManus for providing the glassy carbon electrode used in this research.

References

[1] G. Pleßmann, M. Erdmann, M. Hlusiak, C. Breyer, Global energy storage demand for a 100% renewable electricity supply, Energy Procedia 46 (2014) 22–31. doi:10.1016/j.egypro.2014.01.154.

[2] C. Bussar, M. Moos, R. Alvarez, P. Wolf, T. Thien, H. Chen, Z. Cai, M. Leuthold, D. U. Sauer, A. Moser, Optimal allocation and capacity of energy storage systems in a future european power system with 100% renewable energy generation, Energy Procedia 46 (2014) 40–47. doi:10.1016/j.egypro.2014.01.156.

[3] C. Ponce-de León, A. Frías-Ferrer, J. González-García, D. Szánto, F. C. Walsh, Redox flow cells for energy conversion, Journal of Power Sources 160 (1) (2006) 716–732. doi:10.1016/j.jpowsour.2006.02.095.

[4] R. L. Clarke, B. Dougherty, S. Harrison, P. J. Millington, S. Mohanta, Cerium batteries, US Patent 7,625,663 (Dec. 1 2009).

[5] P. K. Leung, C. Ponce-de Leon, C. T. J. Low, A. Shah, F. C. Walsh, Characterization of a zinc–cerium flow battery, Journal of Power Sources 196 (11) (2011) 5174–5185.

[6] P. K. Leung, C. Ponce-de León, C. T. J. Low, F. C. Walsh, Zinc deposition and dissolution in methanesulfonic acid onto a carbon composite electrode as the negative electrode reactions in a hybrid redox flow battery, Electrochimica Acta 56 (18) (2011) 6536–6546. doi:10.1016/j.electacta.2011.04.111.

[7] P. K. Leung, C. Ponce-de León, C. T. J. Low, F. C. Walsh, Ce(III)/Ce(IV) in methanesulfonic acid as the positive half cell of a redox flow battery,

Electrochimica Acta 56 (5) (2011) 2145–2153. doi:10.1016/j.electacta.2010.12.038.

[8] M. Matheswaran, S. Balaji, S. J. Chung, I. S. Moon, Electro-oxidation kinetics of cerium (III) in nitric acid using divided electrochemical cell for application in the mediated electrochemical oxidation of phenol, Bulletin-korean chemical society 28 (8) (2007) 1329.

[9] R. P. Kreh, R. M. Spotnitz, J. T. Lundquist, Mediated electrochemical synthesis of aromatic aldehydes, ketones, and quinones using ceric methanesulfonate, The Journal of Organic Chemistry 54 (7) (1989) 1526–1531.

[10] Z. Xie, F. Xiong, D. Zhou, Study of the Ce^{3+}/Ce^{4+} redox couple in mixed-acid media (CH_3SO_3H and H_2SO_4) for redox flow battery application, Energy & Fuels 25 (5) (2011) 2399–2404. doi:10.1021/ef200354b.

[11] G. Nikiforidis, W. A. Daoud, Effect of mixed acid media on the positive side of the hybrid zinc-cerium redox flow battery, Electrochimica Acta 141 (2014) 255–262. doi:10.1016/j.electacta.2014.06.142.

[12] S. Peng, N.-F. Wang, X.-J. Wu, S.-Q. Liu, D. Fang, Y.-N. Liu, K.-L. Huang, Vanadium species in CH_3SO_3H and H_2SO_4 mixed acid as the supporting electrolyte for vanadium redox flow battery, International Journal of Electrochemical Science 7 (1) (2012) 643–649.

[13] S. Kim, E. Thomsen, G. Xia, Z. Nie, J. Bao, K. Recknagle, W. Wang, V. Viswanathan, Q. Luo, X. Wei, A. Crawford, G. Coffey, G. Maupin, V. Sprenkle, 1 kW/1 kWh advanced vanadium redox flow battery utilizing mixed acid electrolytes, Journal of Power Sources 237 (2013) 300–309. doi:10.1016/j.jpowsour.2013.02.045.

[14] S. Kim, M. Vijayakumar, W. Wang, J. Zhang, B. Chen, Z. Nie, F. Chen, J. Hu, L. Li, Z. Yang, Chloride supporting electrolytes for all-vanadium redox flow batteries, Physical Chemistry Chemical Physics 13 (40) (2011) 18186. doi:10.1039/c1cp22638j.

[15] P. K. Leung, C. Ponce-de León, F. C. Walsh, An undivided zinc–cerium redox flow battery operating at room temperature (295 k), Electrochemistry Communications 13 (8) (2011) 770–773. doi:10.1016/j.elecom.2011.04.011.

[16] P. K. Leung, C. Ponce-de León, F. C. Walsh, The influence of operational parameters on the performance of an undivided zinc–cerium flow battery, Electrochimica Acta 80 (2012) 7–14.

[17] L. F. Arenas, F. C. Walsh, C. Ponce-de León, The importance of cell geometry and electrolyte properties to the cell potential of zn-ce hybrid flow batteries, Journal of The Electrochemical Society 163 (1) (2016) A5170–A5179.

[18] J. Pan, Y. Wen, J. Cheng, J. Pan, Z. Bai, Y. Yang, Zinc deposition and dissolution in sulfuric acid onto a graphite–resin composite electrode as the negative electrode reactions in acidic zinc-based redox flow batteries, Journal of Applied Electrochemistry 43 (5) (2013) 541–551. doi:10.1007/s10800-013-0538-1.

[19] C. Cachet, R. Wiart, Zinc deposition and passivated hydrogen evolution in highly acidic sulphate electrolytes: Depassivation by nickel impurities (nov 1990). doi:10.1007/bf01019581.

[20] I. Zouari, F. Lapicque, An electrochemical study of zinc deposition in a sulfate medium, Electrochimica Acta 37 (3) (1992) 439–446. doi:10.1016/0013-4686(92)87033-v.

[21] J. Yu, H. Yang, X. Ai, Y. Chen, Effects of anions on the zinc electrodeposition onto glassy-carbon electrode, Russian journal of electrochemistry 38 (3) (2002) 321–325.

[22] G. Trejo, Nucleation and growth of zinc from chloride concentrated solutions, Journal of The Electrochemical Society 145 (12) (1998) 4090. doi:10.1149/1.1838919.

[23] J. Mcbreen, E. Gannon, ChemInform abstract: Electrodeposition of zinc on glassy carbon from zinc chloride and zinc bromide electrolytes, Chemischer Informationsdienst 14 (49) (1983) 47. doi:10.1002/chin.198349021.

[24] L. H. Mendoza-Huízar, C. H. Rios-Reyes, M. G. Gómez-Villegas, Zinc electrodeposition from chloride solutions onto glassy carbon electrode, Journal of the Mexican Chemical Society 53 (4) (2009) 243–247.

[25] G. Nikiforidis, L. Berlouis, D. Hall, D. Hodgson, Evaluation of carbon composite materials for the negative electrode in the zinc–cerium redox flow cell, Journal of Power Sources 206 (2012) 497–503.

[26] H. Nakamura, S. Oue, N. Sogabe, H. Nakano, Effect of chloride ions on the deposition behavior and morphology of zinc at initial stage from electrowinning solution, Journal of MMIJ 131 (5) (2015) 164–169. doi:10.2473/journalofmmij.131.164.

[27] J. Yeager, J. P. Cels, E. Yeager, F. Hovorka, The electrochemistry of nickel i. codeposition of nickel and hydrogen from simple aqueous solutions, Journal of the electrochemical society 106 (4) (1959) 328–336.

[28] Z. Nagy, Chloride ion catalysis of the copper deposition reaction, Journal of The Electrochemical Society 142 (6) (1995) L87. doi:10.1149/1.2044254.

[29] R. L. Pecsok, J. J. Lingane, Polarography of chromium (II), Journal of the American Chemical Society 72 (1) (1950) 189–193.

[30] J. Heyrovský, Retarded electrodeposition of metals studied oscillographically with mercury capillary electrodes, Discussions of the Faraday Society 1 (1947) 212. doi:10.1039/df9470100212.

[31] J. Vazquez-Arenas, M. Pritzker, Effect of electrolyte and agitation on the anomalous behavior and morphology of electrodeposited Co–Ni alloys, Journal of Solid State Electrochemistry 17 (2) (2012) 419–433. doi:10.1007/s10008-012-1932-z.

[32] V. Gouda, M. Khedr, A. S. El Din, Role of anions in the corrosion and corrosion-inhibition of zinc in aqueous solutions, Corrosion Science 7 (4) (1967) 221–230.

[33] J. Blackledge, N.-S. Hush, Mechanism of the Zn(II)/Zn(Hg) exchange: Part 2: catalysis by halide and thiocyanatk ions, Journal of Electroanalytical Chemistry (1959) 5 (6) (1963) 435–449.

[34] E. Ahlberg, H. Anderson, Simulating impedance spectra from a mechanistic point of view: application to zinc dissolution, Acta Chemica Scandinavica(Denmark) 46 (1) (1992) 15–24.

[35] G. Nikiforidis, W. A. Daoud, Indium modified graphite electrodes on highly zinc containing methanesulfonate electrolyte for zinc-cerium redox flow battery, Electrochimica Acta 168 (2015) 394–402.

[36] S. Ranganathan, T.-C. Kuo, R. L. McCreery, Facile preparation of active glassy carbon electrodes with activated carbon and organic solvents, Analytical Chemistry 71 (16) (1999) 3574–3580. doi:10.1021/ac981386n.

[37] M. D. Gernon, M. Wu, T. Buszta, P. Janney, Environmental benefits of methanesulfonic acid, Green Chemistry 1 (3) (1999) 127–140. doi:10.1039/a900157c.

[38] Q. B. Zhang, Y. Hua, Effect of Mn^{2+} ions on the electrodeposition of zinc from acidic sulphate solutions, Hydrometallurgy 99 (3-4) (2009) 249–254. doi:10.1016/j.hydromet.2009.09.002.

[39] R. de Levie, Anion bridging and anion electrocatalysis on mercury, Journal of The Electrochemical Society 118 (8) (1971) 185C. doi:10.1149/1.2408333.

[40] L. G. Sillén, A. E. Martell, Stability constants of metallic-ion complexes, Soil Science 100 (1) (1965) 74. doi:10.1097/00010694-196507000-00026.

[41] M. Capelato, J. Nobrega, E. Neves, Complexing power of alkanesulfonate ions: the lead-methanesulfonate syste, Journal of Applied Electrochemistry 25 (4) (1995) 74. doi:10.1007/bf00249661.

[42] F. I. Danilov, I. V. Sknar, Y. E. Sknar, Kinetics of nickel electroplating from methanesulfonate electrolyte, Russian Journal of Electrochemistry 47 (9) (2011) 1035–1042. doi:10.1134/s1023193511090114.

[43] P. K. Leung, C. Ponce-de León, F. Recio, P. Herrasti, F. C. Walsh, Corrosion of the zinc negative electrode of zinc–cerium hybrid redox flow batteries in methanesulfonic acid, Journal of Applied Electrochemistry 44 (9) (2014) 1025–1035.

[44] D. Baik, D. Fray, Electrodeposition of zinc from high acid zinc chloride solutions, Journal of applied electrochemistry 31 (10) (2001) 1141–1147.

[45] G. Nikiforidis, L. Berlouis, D. Hall, D. Hodgson, A study of different carbon composite materials for the negative half-cell reaction of the zinc cerium hybrid redox flow cell, Electrochimica Acta 113 (2013) 412–423.

[46] V. G. Levich, Physicochemical hydrodynamics, Prentice hall, 1962.

[47] E. B. Budevski, Deposition and dissolution of metals and alloys. part a: Electrocrystallization, in: Comprehensive treatise of electrochemistry, Springer, 1983, pp. 399–450.

[48] Q. B. Zhang, Y. X. Hua, T. G. Dong, D. G. Zhou, Effects of temperature and current density on zinc electrodeposition from acidic sulfate electrolyte with [BMIM] HSO_4 as additive, Journal of applied electrochemistry 39 (8) (2009) 1207.